



University of Birmingham

Synthesis of silver nanostructures for biological and environmental applications

By Adwait P.Suratkar

**Department of Geography Earth and Environmental
Sciences**

UNIVERSITY OF
BIRMINGHAM

University of Birmingham Research Archive

e-theses repository

This unpublished thesis/dissertation is copyright of the author and/or third parties. The intellectual property rights of the author or third parties in respect of this work are as defined by The Copyright Designs and Patents Act 1988 or as modified by any successor legislation.

Any use made of information contained in this thesis/dissertation must be in accordance with that legislation and must be properly acknowledged. Further distribution or reproduction in any format is prohibited without the permission of the copyright holder.

Table of Contents

Sl.No	Contents	Page
1	List of figures	5-7
2	List of tables	7
3	Abstract, Aim	8
4	Chapter 1: Introduction	9-24
5	Chapter 2: Instrumentation	24-48
6	Chapter 3: Materials and methods	49-57
7	Chapter 4: Results	57-75
8	Chapter 5: Discussion	76-82
9	Chapter 6: Conclusion	83-84
10	Future work	85-86
10	References	87-93

List of Figures

Sl. No	Figure number
1	Figure 1
2	Figure 1a
3	Figure 1b
4	Figure 1c
5	Figure 1d
6	Figure 2.1.1 (a)
7	Figure 2.1.1 (b)

8	Figure 2.1.2 (a)
9	Figure 2.2.2 (a)
10	Figure 2.2.3 (a)
11	Figure 2.2.4 (a)
12	Figure 2.2.5 (a)
13	Figure 2.3 (a)
14	Figure 2.3 (b)
15	Figure 3(a)
16	Figure 4.1.1 (a)
17	Figure 4.1.2 (a)
18	Figure 4.1.2 (b)
19	Figure 4.1.2 (c)
20	Figure 4.1.2 (d)
21	Figure 4.1.2 (d)
22	Figure 4.1.2 (e)
23	Figure 4.1.2 (f)
24	Figure 4.1.2 (g)
25	Figure 4.1.2 (h)
26	Figure 4.1.3 (a)
27	Figure 4.1.3 (b)
28	Figure 4.1.3 (c)
29	Figure 4.1.3 (d)
30	Figure 4.1.3 (e)
31	Figure 4.1.3 (g)
32	Figure 4.1.3 (h)
33	Figure 4.1.3 (i)

34	Figure 4.1.3 (j)
35	Figure 4.1.3 (k)
36	Figure 4.1.4 (a)
37	Figure 4.1.4 (b)
38	Figure 4.1.4 (c)
39	Figure 4.1.4 (d)
40	Figure 4.1.4 (e)
41	Figure 4.1.4 (f)
42	Figure 4.2.1 (a)
43	Figure 4.2.2 (a)
44	Figure 4.2.2 (b)
45	Figure 4.2.2 (c)
46	Figure 4.2.2 (d)
47	Figure 4.2.2 (e)
48	Figure 4.2.2 (f)
49	Figure 4.2.2 (g)
50	Figure 4.4.2 (h)
51	Figure 4.2.2 (i)
52	Figure 4.2.2 (j)
53	Figure 4.2.2 (k)
54	Figure 4.2.2 (l)
55	Figure 4.2.2 (m)
56	Figure 4.2.2 (n)
57	Figure 4.2.2 (o)
58	Figure 4.4.2 (p)
59	Figure 4.2.2 (q)

60	Figure 4.2.2 (r)
61	Figure 4.3 (a)
62	Figure 4.3 (b)
63	Figure 5(a)
64	Figure 5(b)
65	Figure 5(c)
66	Figure 5(d)
67	Figure 5(e)
68	Figure 5(f)
69	Figure 5(g)

List of tables

Sl.No	Table number
1	Table 3.1.1 (a)
2	Table 3.1.1 (b)
3	Table 3.1.1 (c)
4	Table 3.3 (a)

Abstract

"Nanotechnology is probably, as a phenomenon, the single most important new emerging force in technology." - Charlie Harris, CEO, Harris & Harris Group

As the above quote suggests nanotechnology is not only a technology it is a phenomenon that has taken science to cutting edge technology. Nanotechnology has opened a new era of science where scientists can manipulate at nano meter scale. Nanoparticles are applied in almost all walks of life ranging from cosmetics to health and medical diagnostics (Gupta K.A 2005), ceramics (G. Aharon 2007).

In a project concerning nanoparticles there are three important phases, synthesis phase, characterization phase and application phase. In the synthesis phase nanoparticles are synthesised using various chemical and physical methods that usually involve a surfactant, capping agent and a reducing agent. In recent years there has been a lot of interest in synthesizing nanoparticles of various shapes ranging from cubes, rods, triangles and prisms. In this project we will be focusing on the synthesis of silver nanoparticles, which have a characteristic quadrupole surface plasmon mode and has therefore found itself applicable in Surface Enhanced Raman spectroscopy (Sherry J.L 2006), for single molecule detection. In the project we will also look at the stability of nanoparticles in biological and ecotoxicological media. We will be using Uv-Vis spectroscopy for the analysis of the results.

Aim

The aim of this project is to synthesize silver nanoparticles of triangular or prism shape. The nanoparticles will be characterized using zetasizer nanoseries, UV-Vis-spectroscopy and AFM. Before testing the toxicity of the nanoparticles on different cell lines, their stability will be tested on biological media.

Chapter 1: Introduction

Nanoparticles are particles that have at least one dimension between one and hundred nanometres. Nanoparticles have a unique position between atoms and bulk material giving them unique physical chemical and optical properties like, quantum effects (Li H. W 2003; Volokitin Y 1996; Borgohain. K 2000) that are only possible due to their property of electron confinement; this is ability unique to nanoparticles, property of photoluminescence shown by quantum dots such as CdS and many metal nanoclusters (Jin .R et al 2010) such as those of gold and silver (Maretti L et al 2009). Another example is the ability of anisotropic nanoparticles such as rods, and triangular prisms to show multiple scattering peaks in the visible region of the electromagnetic spectrum. These properties make them a right candidate for research and development. Properties of nanoparticles are governed by physical factors such as size, shape, chemical composition and structure. These properties can be tailored according to the application of the nanoparticle.

Recently there has been a great interest of nanoparticles in biological applications, for example silver nanoparticles have been used as antibacterial (Lok N.C 2007; Baker C 2005; Morones R.J 2005) and antimicrobial agent, Iron oxide nanoparticles have been used in medical diagnostics (Gupta K.A 2005), and titanium dioxide (TiO₂) nanoparticles (Wei Q 2007; Yang H 2004) have been used extensively as uv-blocking agents in cosmetics. Metallic nanorods are used in chemical sensing and bio-imaging (Murphy C.J 2007).

There are two types of nanoparticles, isotropic nanoparticles and anisotropic nanoparticles. Spherical nanoparticles are considered as isotropic and non-spherical (rods, triangular shape and wires) are considered as anisotropic nanoparticles. When the shape of a nanoparticle changes its properties change, for example a silver nanoparticle that is spherical in shape will absorb in the ultra-violet region of the electromagnetic spectrum, but

when the shape of the silver nanoparticle changes to prism, it absorbs light in the visible and near infrared region. The scientific community has seen significant progress in the synthesis of nanoparticles of various shapes include mainly cubes (Sun.Y 2002), triangular prisms (Métraux G. S 2005), plates (Goebel J 2012; Zhang Q 2011) and metallic nanorods (Xia .Y 2003; Busbee B.D 2003), between the years 2000 to 2012. There have some really good articles written by Xia Y and Mirkin C.A on the synthesis of anisotropic nanoparticles, especially the synthesis of gold nanoprisms by Mirkin C.A 2001; 2003; 2005; 2007, has been a highly cited and appreciated article.

Spherical nanoparticles of gold where first developed by Michael Faraday in 1850s through the reduction of gold chloride in water along with phosphorus to produce a ruby red colour solution of gold nanoparticles. 150 years later there has been some remarkable progress in solution based synthesis of nanoparticles. Monodispersity still remains a challenge as most of the methods have synthesized nanoparticles that are polydispersed in nature. There have been many solution based methods developed to synthesize various shapes of these nanoparticles, what is interesting to note is that, these nanoparticles deviate from Wuff's theorem (Wuff 1901) making the synthesis tricky and difficult to achieve. There have been many solution based methods developed over the years to synthesize gold and silver nanoparticles.

There are two types of nanoparticles organic nanoparticles and metal nanoparticles. Metal nanoparticles consist of iron oxide nanoparticles, cerium dioxide nanoparticles, gold nanoparticles, silver etc. Organic nanoparticles mainly consist of polystyrene nanoparticles, PEP nanoparticles, etc. If we compare organic and inorganic synthesis of nanoparticles, in organic synthesis a number of complex molecules can be attached to polymer and numerous organic molecules can be designed. But there is a limit to attached assembly of metal atoms in a nanoparticle. There is a really interesting point to be noted here, compared to organic synthesis, the chemical reaction involved in the synthesis of metal nanoparticles is very simple and can be found in elementary chemistry text book, what is tricky and difficult

to understand is the process of nucleation, growth and birth of nanoparticles. Before we could further understand the synthesis of anisotropic nanoparticles, it is important to know the complex physics and chemistry behind the birth of nanoparticles, how their shape can be manipulated using the knowledge of thermodynamics, reaction kinetics and by the appropriate selection of capping agents. This is important because it will give the reader a correct perspective of how nanoparticles evolve into various shapes.

At the current stage of scientific understanding synthesis of nanoparticles of various shapes is more of a fine art than a well-defined process.

There are three major steps in the growth of nanoparticles:

- (i) The process of nucleation
- (ii) The process of nuclei to seed formation
- (iii) Birth of nanoparticles from seeds.

1.1 The process of nucleation.

Nucleation is the first phase of nanoparticle synthesis process. Nucleation is a phase where ions are converted into atoms. In a typical synthesis of nanoparticles the metal precursor is decomposed to atoms which are building blocks for the growth of metal nanoparticle. It is not exactly clear how nanoparticles are born out of atoms, but the overall process is called as nucleation. Two theories have been proposed to understand the process of nucleation.

Theory 1: In the year 1950 LaMer and co-workers have extensively worked on the nucleation process (Figure 1) and the growth of nanoparticles. According to their theory the concentration of nanoparticles increases as the reaction progresses and the precursor is decomposed. Once the concentration of the atoms reach its limit (point of supersaturation) they begin to come together in the form of small clusters and there begins the process of

nucleation and nanoparticle growth. If the level of supersaturation is not reached then the event of nucleation will not occur and as a result of that a nanoparticle will not be formed.

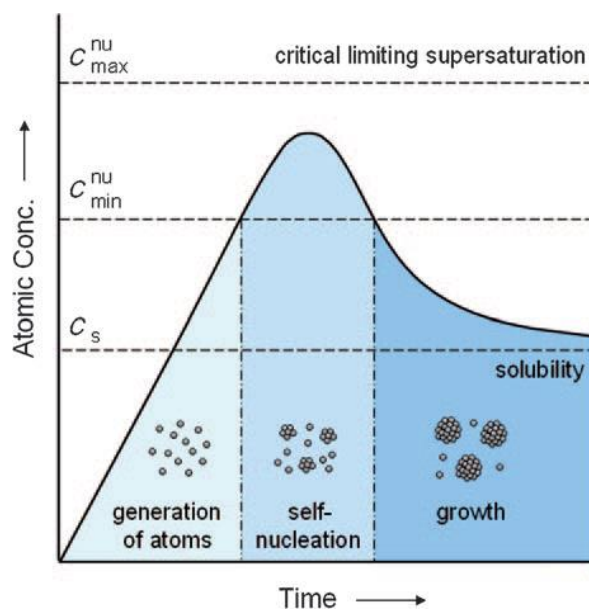


Figure 1. It is a graph that shows atomic concentration versus time, modified by Y.Xia 2009, from LaMer V.K 1950 American Chemical Society.

Let us understand this theory by taking an example of a simple reaction (refer to equation (1)) involving the synthesis of gold nanoparticles using chloroauric acid as the precursor (HAuCl_4) and sodium borohydride as a reducing agent, the tetrahydroborate ion (BH_4^-) is responsible for the reduction of AuCl_4^- to gold nanoparticles. Using the theory given by LaMer and co-workers (Illustrated in Figure 1) the Au^{3+} ions will be reduced to (Au^0) gold atoms that will self-nucleate to form nanoparticles, which will grow in size until there is an equilibrium reached between the surface atoms of the nanoparticle and the atoms present in the solution, this phase is called as the growth phase.

Theory 2: The second theory concerns the reduction process. This theory is different from the LaMer's model because in the reduction process the atomic species born is in a lower reduction state than the metal precursor. It is still unclear whether the metal precursor is first reduced to zero-valent ions and then the atoms come together to form the nanoparticles or whether ions come together before they are reduced to atoms. Based on the computer simulation studies it has been confirmed that nuclei come together and form initial clusters

without undergoing zero valent metal atomic state. A good example to understand this process is the formation of Pt dimers and trimers directly from platinum chloride (PtCl_4) without their reduction into zero valent Pt. According to by L.C. Ciacchi et al 2003, Pt dimer and trimer stabilized by Cl- ligand is formed directly from a complex PtCl_4 and water through the addition of an electron and loss of chloride ion. These partially reduced dimers and trimers are the building blocks for a cluster which produce the nanoparticles. The clusters are formed by the detachment of (water) ligand from the dimer. Once this process occurs the clusters goes through a phase of accelerated growth which is known as autocatalytic growth phase. In this phase the cluster grows quickly into a nanoparticle. This process has been observed for many metal nanoparticle systems (Z.Y. Huang et al 1993, E.E. Finney et al 2008, H.W.Roesky et al 2006).

1.2 Process of Nuclei to seeds formation.

Once the cluster of atoms grows and reaches a critical diameter, fluctuations in structure of the cluster become energetically difficult. As a result the cluster will have a well-defined structure. This point in the initial phase of a reaction is the birth phase of seed. Seed is important as it is a bridge that links together nuclei and nanocrystals. There are different types of seeds based on the shape of the cluster, such as (i) single-crystal, (ii) single twinned; and (iii) multi-twinned seeds (refer to figure 1a). It is possible that multiple shapes of cluster can co-exist in a particular synthesis process. If we wish to obtain nanoparticles of a particular shape then it is important to control the population of seeds with various internal structures. The population of seeds is controlled during the early synthesis phase of a reaction, through a combination of thermodynamic and kinetic control of the reaction. This is because the formation and stability of structures is dependent on thermodynamic and kinetic factors, to sum up the above; the number of differently structured seeds can be determined by the statistical thermodynamics of free energies of various seeds and at the same time controlling kinetically the addition and conversion of metal ions to metal atoms. Seed

population can also be controlled through a process known as oxidative etching. The role played by the above processes will be discussed extensively in the following section.

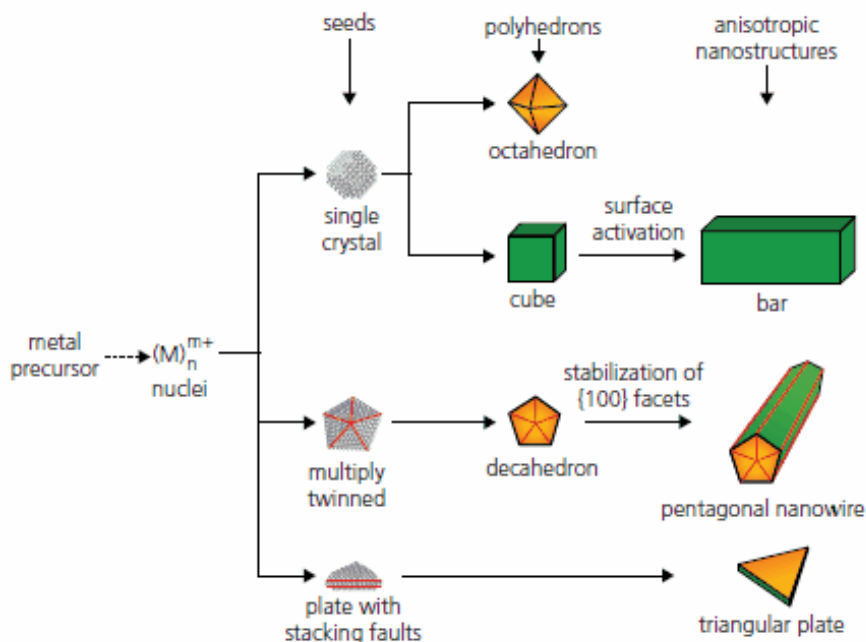


Figure 1a, illustrates the formation of seeds from metal precursor, there are three type of seeds single crystal, multi-twinned, plate with stacking faults.

Reference: Y.Xia 2011, Material Matters, Vol 4 article 1. Sigma-Aldrich

1.3 Controlling the thermodynamics of the reaction.

When a chemical reaction is under complete thermodynamic control, the highest proportion of the product produced will be the most stable product of the reaction. To find out what will be the most stable product in a chemical reaction. Let us take the example of single-crystal seed which can be explained by Wulff's theorem (Wulff's theorem: tries to minimize the total interfacial surface energy of a given system with given volume). The interfacial free energy can be defined as the energy required in creating a unit area of new surface, where G is the free energy and A is the surface area.

$$\gamma = (\Delta G / \Delta A)_{n_i, T, P} \quad (1) \text{ (Xia Y 2009)}$$

When a new seed is formed the crystal structure is broken due to the loss of bonds on the surface of the crystal, causing the atom present on the surface of the crystal to get attracted

to the interior, there needs to be a restoring force that pulls the atom back to its surface, we can use this as a simple tool to explain and define the interfacial energy which is given by equation (2) N_b is the bonds broken and ϵ being the bond strength, and p_a being the number of atoms on the surface.

$$\gamma = \frac{1}{2} (N_b \epsilon p_a) \quad (2) \quad (\text{Xia. Y 2009})$$

When the synthesis involves formations of FCC (face centered cubic) structures, the surface energies are given as following: γ [100] facet = $4 (\epsilon/a^2)$, γ [110] facet = $4.24 (\epsilon/a^2)$, γ [111] facet = $3.36 (\epsilon/a^2)$. These facets induce energy sequences in which face [111] requires least energy, than [100] and the highest energy is required by [110] facet. According to this, we can understand that when a single-crystal seed is formed it takes an octahedral shape and it minimizes the total surface energy to expose the [111] facet. Single-crystal seeds have a large surface area, and therefore spherical in shape. These seeds grow to form spherical nanoparticles. Anisotropic shapes can also be formed from these seeds, which mainly include cubes and bar shaped nanoparticles. To form prism or triangular shaped nanoparticles, plate shaped seeds have to be formed with stacking faults illustrated in Figure 1a. The size, shape and population of the seed nanoclusters need not be governed completely by thermodynamics; but reaction kinetics also plays a critical role, which can be experimentally manipulated.

1.4 Reaction Kinetic of typical synthesis.

Reaction kinetics concerns the different components that will be added to the reaction mixture. To achieve spherically shaped nanoparticles it is important that the seeds be single crystal in shape. According to literature if seeds expand and grow rapidly then there are higher chances of producing spherical nanoparticles. To produce nanoparticles or nanocrystal of various shapes it is important that seeds be confined to a smaller shape and that their evolution be slow and not rapid. This means that the reaction needs to be sufficiently slowed down to keep the atomic generation or addition low. Therefore, when the

addition or generation of atoms is low, multi-twinned and plate like seeds appear which are necessary for the generation of anisotropic nanoparticles. Also, by varying the concentration of the precursor (metal salt) and the rate of reduction of the precursor, different seeds can be synthesized.

When the decomposition or the reduction of ions becomes slow, atoms usually form nuclei and seeds through a process called random hexagonal closed packing (RHCP). This is also the case in plate like structures which have stacking of atoms. When a process of synthesis is under kinetically controlled state, the atoms deviate from thermodynamically favoured structures. A good example for this is the formation of plate like structures. Thermodynamically for a plate like seed to be formed, the crystal lattice needs to have a high surface area, but the defects caused by lattice strain energy are so high, that it makes it impossible to be formed. It is observed that plate like seeds are formed in a solution when the nucleation and growth of the seeds deviate from the laws of thermodynamics.

There are four ways of kinetically controlling the structures of nanoparticles, (i) Slowing down the decomposition and/or the reduction of the precursor (metal salt) (P.F. Ho 2004; Y.Xia 2007); (ii) Using a weak reducing agent (Y.Xia 2006; Y.Xiong 2006; B.Lim 2008); (iii) Combining a reduction process with a oxidation process (Y.Chiong 2005); (iv) Taking advantage of the process of Ostwald ripening (Y.Sun 2003; Y.Sun 2005). Also lowering the concentration of the metal ions and atoms in the solution will led to the addition of atoms to the edge of the plate like cluster and form triangular plates and not form polyhedral structures.

1.5 The process of Oxidative Etching.

The process of etching is an oxidative process where in the metal atoms are converted into metal ions by the process of oxidation in the presence of oxygen and other oxidizing agents. We may think that how oxygen that is present through the process of synthesis in the form of air does not oxidize the reactants. This is because oxygen is molecular in nature, in a

solution when oxygen is added in combination with a ligand (ex: H_2O_2) the resulting mixture is a powerful etching agent. Single or multi-twinned seeds are more prone to oxidative etching than spherical seeds for a simple reason that they have more defects and edges on their surface.

According to an experiment conducted by Y.Xia 2004, in a polyol synthesis of silver nanoparticles, the multi-twinned seeds can be completely removed from the solution by the addition of chloride ion (Cl^-), resulting in the synthesis of nanoparticles of various shapes.

Nanocrystals of various shapes of the metal Ag, Pd and Rh have been synthesized by B.Wiley et al 2006, 2007, 2004; and Y.Xiong 2005a, 2005b using oxidative etching, for the etching process to occur successfully and to get nanoparticles of monodispersed nanoparticles of desired shape it is important that counter ions be introduced into the reaction mixture. An example for this can be taken by research experiments done by Y.Xia et al, and Y.Xiong et al, in this experiment polyol synthesis of silver nanoparticles was done in the absence of oxygen and presence of Argon gas, there was evolution of silver nanowires. But when O_2 and Cl^- were both added to the solution simultaneously, polyhedral nanoparticles were evolved. We can make following conclusions from the above experiments: (i) diminishing O_2 from the reaction and introducing an inert gas can produce seeds that are multi twinned, (ii) blocking the seeds with capping agents and introducing oxygen scavengers like copper and iron can produce seeds of various shapes, and produce wires and rods of desired shape and size.

It is interesting to note that the presence of ions, intrinsic to the reaction can also play a role in shaping the nanoparticles, like the metal precursors in the synthesis can also oxidatively etch on the surface of the budding nanoparticle seed. A good example for this is the precursor for Au synthesis HAuCl_4 which contains Cl^- which is important component of oxidative etching. Another example for this condition is described by B.Wiley et al (2005) in the polyol synthesis of Pd which involves oxidative etching by Cl^- . It is important therefore to

keep knowledge of such small impurities and to nanoparticles must be filtered after their synthesis, these points are important when synthesis of nanoparticles is scaled up.

1.6 Formation of nanoparticles from Seeds.

Once seeds are formed atoms are added to them to form nanoparticles of various shapes and sizes. However the whole process is not easy and it is very difficult to document the events taking place in real time. According to chemical analysis atoms are added to the crystal surface until there are no more sites for their incorporation. There are two important factors that need to be addressed when studying the growth of nanoparticles; (i) decrease in the bulk energy that favours the growth of nanoparticles; and (ii) increase in surface energy which favours the dissolution of nanoparticles. The two factors compete with each other during the growth phase of nanoparticles. Transmission electron microscopy has been an important tool in studying the growth of nanoparticles, using this there has been established a one to one relationship between the initial seed and the final nanoparticle growing out of it. It is still difficult to study the complete growth process of nanoparticles.

Single crystal seeds give rise to polyhedrons which are the intermediate structures. According to research done by Y.Xia 2009, single crystal seed give rise to octahedral, cuboctahedral and cube shaped nanoparticles. When further growth is allowed in these nanoparticles they give rise to octagonal rods and rectangular rods, with [100] facets exposed. Single twinned seeds give rise to pyramid and bipyramid shaped nanoparticles. Multi-twinned seeds give rise to decahedron and icosahedrons shaped nanoparticles. When the [100] facet is allowed to stabilize, we get pentagonal rods. Plate like seeds gives rise to nano-plates and hexagonal shaped nanoparticles. This is the physics behind the synthesis of not only nanoparticles of various shapes but also of nanoparticles in general.

1.7 Silver Nanoprisms

Silver nanoparticles of various shapes have been observed under electron microscope synthesized using various methods, these include rods, wires, cones, disks, plates and other

interesting structures. Silver nanorods can be synthesized by thermal, photochemical and surfactant based method. Some of these techniques have been very successful in controlling the aspect ratio and the size of the nanoparticles, and have had many applications in electronics and photonic based applications. The years 2005 to 2010 have seen the growth of a new class of nanoparticles, which are pyramids, and cubic in structure. Y.Xia and his co-workers should be credited for their work in silver nanoprisms. An interesting aspect of these nanoparticles is that they show multiple Plasmon modes, and absorb light between 600 to 1000 nm, most of this absorption is because of the shape and size of the nanoparticles. Current research is looking to increase the yield of nanoprisms. Silver nanoprisms or nanoplates are platonic shapes of silver which have a flat triangular base and desired thickness (refer to figure 1b). They also have a very large aspect ratio. Depending on the thickness, height and aspect ratios, they can be categorized as Triangles, plates and other complex structures.

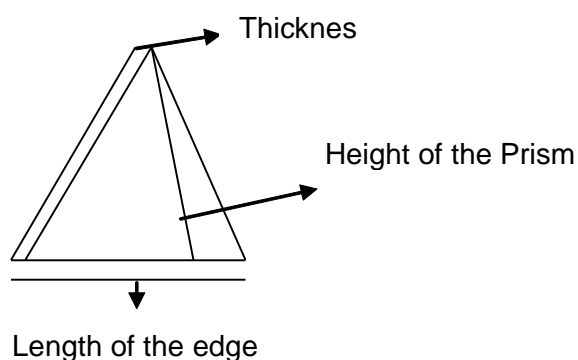


Figure 1b. shows the dimensions of prism

Silver nanoprisms have large edges that play a vital role in the optical properties of the nanoparticles. During the process of prism formation the process of “rounding” can occur which can give rise to circular discs like plates. In the past few years there have been several methods developed to design the dimensions of the silver nanoprisms.

Silver nanoprisms or nanostructures in general have a lattice structure of FCC (face centered cubic). When triangular, hexagonal or spherical nanoparticles are synthesized, they have a [111] crystal faces, with [100], [110] facets. The common features of Ag and Au nanoprisms are that they all have size tunable surface plasmon resonance. A typical UV-Vis spectrum of silver nanoprisms would show the nanoparticles absorbing in the visible region and the broad peak in the NIR infrared region. There are several ways to synthesize silver

nanoprisms, though most of methods are surfactant based. Some of the many ways synthesizing silver nanoprisms are (i) photochemical synthesis of nanoprisms; (ii) synthesis under visible light; (iii) thermal synthesis; (iv) synthesis under UV-light; (v) biosynthesis of nanoprisms.

1.7.1 Photochemical Synthesis of nanoprisms.

As the name suggests in photochemical synthesis of nanoprisms light is used as the fundamental medium to convert the seed particles into nanoprisms, and control their shape and optical properties. There have been many methods developed to synthesize nanoprism in the presence of light. Some of them include the synthesis under visible light, UV-light and radiolysis. In the following section we will look at the synthesis of nanoprisms under various conditions of light.

1.7.2 Synthesis under visible light.

In this section we will look at the synthesis of silver nanoprisms under light ranging from 300 nm to 800 nm. This was first reported by C.Mirkin et al in 2001, when they synthesized silver nanotriangles from bis(p-sulfonatophenyl)phenylphosphine dipotassium (BSPP) salt using fluorescent light. Silver nanoprisms of 100 nm have been synthesized by C.Mirkin et al using fluorescent light. The important part of the synthesis is that it can be turned on and off by just switching on and switching off the light source. When the nanoparticles are analysed on a UV-Vis spectrophotometer, there are three important peaks those need to be noted. The first peak is at 670 to 700 nm due to the in-plane dipole resonance, second is between 400 to 450 nm due to in-plane quadrupole resonance. Third is a sharp peak at 331nm due to out-of-plane quadrupole resonance. These peaks have been theoretically calculated and experimentally proved by C.Mirkin et al, Schatz and co-workers in their collaborative work.

According to the experiments done by C.Mirkin et al, when silver nanoparticles that are spherical in nature are excited by light of single wavelength 550 nm, results in a solution of silver nanoprisms with two size distributions, one set of them have an edge length of 70 nm

and the other set has an edge length of 150 nm. There are also variations in the prism thickness and plasmon excitation. Therefore by varying the wavelength of the incoming radiation, the edge length and the thickness can be varied.

When there is an additional capping agent added in the form of tri-sodium citrate, triangular disc shaped nanoparticles are retrieved from spherical seeds. The SPR slowly shifts from 400nm at the beginning of the reaction to three distinct peaks at 331nm, 450 nm and 600 nm. According to Brus et al, the shape of the nanoparticles changes with the exposure time, i.e, the amount of silver nanoprisms are greatly increased as the exposure time is increased. With nanoparticles attaining longer wavelength as the shape becomes more disk like.

Let us now understand the mechanism by which silver nanoprisms are formed photochemically (illustrates in Figure 1c). The ingredients in this reaction are AgNO₃ the precursor, BSPP which acts as the capping agent along with citrate. The reaction begins with the reduction of silver nitrate by sodium borohydride, and there is a formation of spherical silver nanoparticle seeds having Uv-Vis spectra at 400 nm. When the light passes through the solution of silver nanoparticles, it excites the surface plasmons creating electron hole pairs on the surface of the nanoparticle. The further reaction is the reduction of silver ions by tri-sodium citrate, and the oxidative dissolution of Ag nanoparticles by oxygen. The role played BSPP is to allow the dissolution of Ag ions by complexing with Ag nanoparticles. It was further suggested by Brus et al that there is face selective reduction of Ag ions into nanoprisms. The reaction is as follows:

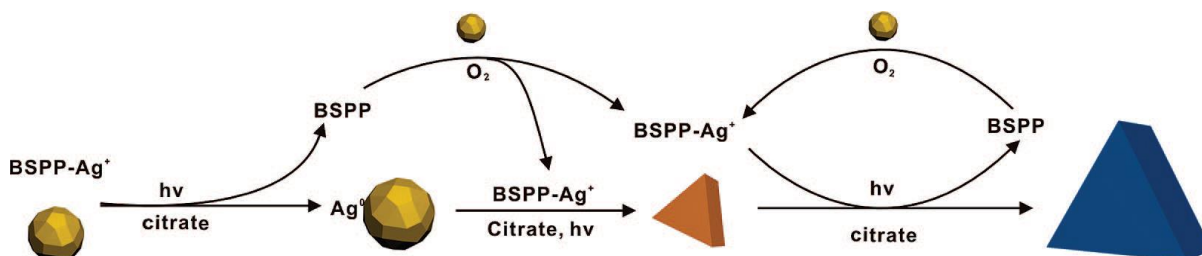


Figure 1c photochemical synthesis of nanoprisms using BSPP Ref: Chad A. Mirkin **J. AM. CHEM. SOC.** **2008**, *130*, 8337–8344

1.7.3 Synthesis under UV light:

Apart from synthesis of silver nanoprisms under visible light, they can also be synthesized using UV-light. The UV-light is used as a source of energy to provide heat to the reaction so that nanoprisms can be formed from spherical nanoparticles. In some of the synthesis done by Y.Takeuchi 2001, UV-light was used to generate reactive species to produce metal atoms from metal ions. This synthesis is unique because, in this synthesis surface plasmons are not formed by the metal atoms. In a typical reaction mixture, there is the precursor AgNO_3 and a capping agent in the form of (nicotinic acid, formic acid, and pyrimidine). The mixture is boiled in the presence of UV-light of about 400 nm. The theory behind the formation of silver nanoprisms is that the capping agents like pyrimidine selectively bind to certain surfaces of the nanoparticles, thereby dictating the shape to prism like.

Silver nanoprisms can be also synthesized by radiolysis, as shown by Delcourt et al, in the presence of suitable organic surfactant, like EDTA. In a typical synthesis, silver nanoprisms were obtained by adding a solution of silver sulphate and EDTA, and 2-propanol, and exposing the solution to several krad's of radiation. The process is similar to other photochemical methods, where initially spherical seeds are formed which are converted to silver nanoprisms by surfactant directed growth of the nanoparticle.

To summarize the synthesis of silver nanostructures using photochemical methods, the critical parameters are the wavelength of the light which decide the edge length and the thickness of the nanoprism. The growth of the nanoprisms involves blocking of specific crystal faces by the surfactant or the capping agent and the production reactive oxygen species by incoming radiations.

1.7.4 Thermal Synthesis:

After photochemical methods we will now move on to look at some the thermal methods developed over the years to synthesize triangular structures of silver. In a general synthesis protocol (C.Mirkin 2005) sodium citrate is mixed with silver nitrate, PVP or BSPP can be used as the surfactant for this reaction and sodium borohydride is used as the reducing agent and hydrogen peroxide is used as the oxidative etchant. The concentration of tri sodium citrate is varied from 1mM to 30mM, the end product is sea blue colour solution of silver prisms. According to the research conducted by Mirkin et al, the amount of sodium borohydride decides the thickness of the prism, which is varied from 100 μ l to 250 μ l.

The important point to be noted about this reaction is that unlike the photochemical and the chemical route in this reaction monodispersed nanoparticle of silver can be obtained. According to the research conducted by Mirkin et al, the amount of sodium borohydride decides the thickness of the prism, which is varied from 100 μ l to 250 μ l.

1.7.5 Other anisotropic nanostructures of silver:

Apart from silver nanoprism, Murphy et al have also developed a chemical surfactant mediated method to synthesis silver nanorods, and nanowires. These methods produce a typical nanorod of 50 to 200 nm. It is a seed mediated method, which involves the generation of silver nanorods from seed nanoparticles. Generally the seed nanoparticles are spherical in nature and they are synthesized by reduction of silver nitrate in the presence of sodium borohydride and tri sodium citrate. The size of the seed nanoparticles varies from 4nm to 18nm depending on the type of surfactant and capping agent used. Usually the surfactant used is cetyltrimethylammonium bromide (CTAB). Once the seed nanoparticles are prepared they are further reduced by using Ascorbic acid which acts as a reducing agent. In the end 1M sodium hydroxide is added to the above solution, the concentration of NaOH is varied from 100 μ l to 1ml. A general trend that is noticed is that as the concentration of NaOH is increased, the length of the silver nanorod increases and at a concentration of 1ml silver nanowires are obtained (N.R.Jana 2001)

Figure 1d on the right illustrates silver nanowires, the length and aspect ratio of the wires can be controlled by varying the concentration of surfactant, the reducing agent and the surface directing agent. Silver nanowires have been first developed by C.J Murphy group in 2001. After their synthesis in 2001 they have been extensively used in electronic and photovoltaic industry. Nanowires of several metals like, Titanium dioxide, gold, and other transition metals nanowires have application in paint and textile industry.



Figure 1d silver nanowires Ref: Nikhil R. Jana (2001) Chem. Commun., 2001, 617–618,

Chapter 2: Instruments

2.1 DLS Nano zetasizer

In nanotechnology, synthesis of nanoparticles plays a critical role in the entire process. It decides the mode of characterization and the application of the nanoparticles. The main aim during the synthesis of nanoparticles is to control the shape, size and the zeta potential of the nanoparticles. To see if the desired shape is obtained, Uv-Vis-spectroscopy is used. To monitor the zeta potential and the size of the nanoparticle an instrument called nano zetasizer is used. It is a very easy tool used to determine the approximate shape of the nanoparticle. Zeta potential is important because using it the stability of the nanoparticle in the solution can be obtained, this is critical for the further studies of the nanoparticle. The DLS in the nano zetasizer stands for Dynamic Light Scattering (DLS). The process is also called as photon correlation spectroscopy (PCS) as light has been used as the principle medium to illuminate the nanoparticles. The zetasizer has pre-programmed optics, precise temperature control settings and methods that produce accurate and reproducible results, key parameters like mobility, pH and concentration can be calculated. The DLS nano zetasizer uses standard operating procedures (SOPS) to make the measurement. DLS finds its application in bio-nanotechnology, nanotechnology and protein purification and mobility studies, the instrument can also be used to study the melting point of proteins. The tool is simple, handy and very easy to use. In the next two to three pages we will look at the principle, working and the design of the instrument.

2.1.1 Principle of DLS Nano zetasizer:

Nano zetasizer works on the principle scattering of light by Particles in a solution are moving randomly, and they are in a state of continuous motion. This process is called Brownian motion. The instrument performs its functions using a process called Dynamic Light Scattering (DLS), and measures the Brownian motion of the nanoparticles under the influence of laser light. The DLS nano zetasizer correlates the size of the nanoparticles to

the Brownian motion using the process of photon correlation spectroscopy (PCS), this analyses the fluctuations in the intensity of the scattered laser light. The size of the nanoparticles is calculated using the hydrodynamic diameter of the particle. The scattering of light is based on two principle theories, the Rayleigh scattering and Mie theory.

Consider a nanoparticle being illuminated by a laser light of certain intensity. What we observe is that the nanoparticle begins to scatter light in all directions. If a screen is held on the opposite end, it will get illuminated by the light scattered by the nanoparticle. There will be a particular pattern of light scattering, with dark and light regions. This will be the case of a single nanoparticle. If we replace this with a solution containing millions of nanoparticles, then we will observe complex pattern of dark and light spots. This is because of the interference pattern caused by the laser after interaction with the surface of nanoparticle. The bright areas are those where the scattered light arrives at the screen in same phase, the dark spots are those where the light arrives at the screen in another phase. To define the interference patterns bright that patches are constructive interference and dark patches are destructive interference. The figure 2.1.1 (a) illustrates how the entire process occurs.

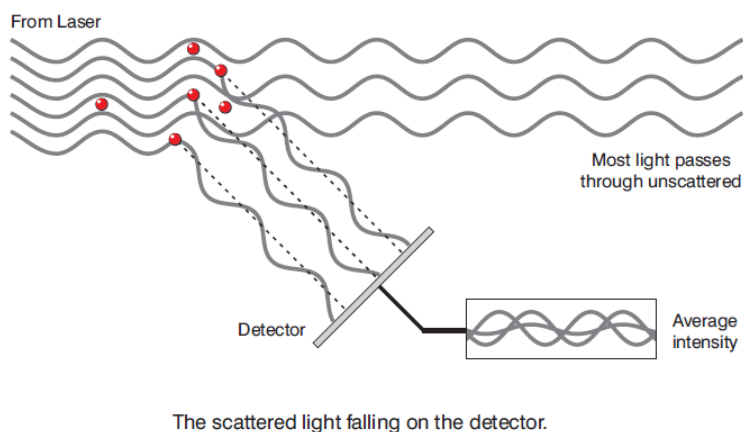


Figure 2.1.1 (a) illustrates the deflected light being picked up by the detector. Reference: Zetasizer Nano Series User Manual MAN 0317 Issue 1.1 Feb.2004, chapter 13, page 13.2

The figure 2.1.1 illustrates the interference pattern for nanoparticles that are in a stationary phase. In case of measuring nanoparticles in a solution, it is important to note that they are

in a state of continuous motion called as the Brownian motion. An important feature of the Brownian motion is that smaller particles move quickly and larger particles move with a slower velocity. As the nanoparticles move continuously, the interference pattern continuously changes and fluctuates. The zetasizer system measures the change in intensity of the fluctuations and uses that data to calculate the size of the nanoparticles.

Using the electrophoretic mobility of the nanoparticles, the instrument also measures the zeta potential of the nanoparticles. The instrument uses a technique called as Laser Doppler velocimetry which uses the Doppler shift in the laser beam to calculate the velocity of particles in a transparent or semi-transparent liquid.

It is important that we first understand the principle behind the double layer surrounding the nanoparticles and the theory behind zeta potential illustrated in figure 2.1.1 (b). A double layer is a layer which surrounds an object when it is exposed to fluid. The electrical double layer consists of counter ions, which is formed due to the net charge every nanoparticle has at its surface. The double layer has two regions, the inner region called as the Stern layer where the ions are strongly bound to the surface of the nanoparticle, and other is on an outer layer referred as the diffuse layer where the ions are loosely bound to the surface. Inside the diffuse layer there is boundary, all the ions within the boundary are firmly bound to the nanoparticle and move along with the nanoparticle due to the force of gravity. But all the ions outside the diffuse layer do not move along with the nanoparticle. The boundary is known as slipping plane. The potential that exists at this layer is called as zeta potential.

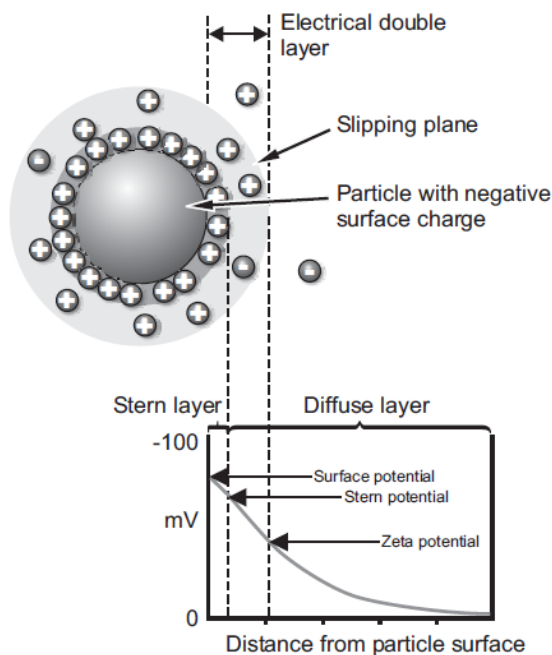


Figure 2.1.1 (b) this image illustrates the ions present around a nanoparticle and also different layers around the surface of the nanoparticle. Reference: Zetasizer Nano Series User Manual MAN 0317 Issue 1.1 Feb.2004, chapter 15, page 15.2

The value of zeta potential describes the stability of the nanoparticles in the solution. The value of the zeta potential also tells us whether the nanoparticles are in a state of aggregation or not. If the zeta potential of the nanoparticles is too high, then the nanoparticles repel each other and don't aggregate. But if the zeta potential is low, the nanoparticles tend to aggregate and flocculate as there is no force stopping them from staying apart. The pH of the solution plays a critical role in variation of the zeta potential of the nanoparticles. To a solution containing nanoparticles acid is added, then the zeta potential of the nanoparticles will be positive in

If to this solution an alkali is added the charge will get neutralized. The point at which the zeta potential is zero with respect to the pH is called as the isoelectric point. At this point the solution is said to be in least stable state. The isoelectric point is important for analysis of proteins.

2.1.2 Working of the Instrument:

The DLS nanosizer is a very compact and simple instrument. The main components the instrument are; (i) laser with a specific wavelength; (ii) A cell used to hold the sample, there are two types of cell, one for size measurement and the other for zeta potential measurement; (iii) A detector used to measure the intensity of the scattered light; (iv) an

attenuator which is used to moderate the intensity of the laser; (v) a digital signal processing correlator; (vi) and a computer to display the correct result.

2.1.2 (A) Cuvettes used for size measurements and zeta potential measurements:

Cuvettes is a small tube of circular or square cross section, sealed at one end, made of plastic, glass or fused quartz and designed to hold samples for spectroscopic experiments. To measure the size in a DLS zetasizer nano series, there are several type of cuvettes available, most of the cuvettes are made of glass and silica. The main function of the cuvettes is to make process as easy and accurate as possible, let us now look at some of the cuvettes available:

For size and molecular weight measurement:

- (1) Quartz flow cell: this is the most basic type of cell used to measure size and intensity of nanoparticles in a solution.
- (2) 12 mm glass cell: this cell is made of glass and is used for size and zeta potential measurement. The advantage of using this cell is that it can be used for aqueous and non-aqueous solvents.
- (3) 12 mm square polystyrene cuvettes: These are cuvettes made of a polymer called as polystyrene. They are used to measure the size and the molecular weight of a substance in a solution.
- (4) Disposable solvent resistant micro-cuvette: this is cuvettes used for very accurate and sensitive measurements of size , the unique feature of this cuvette is that it is used only for 173° backscatter detection, i.e only for those instruments in which the angle of back scatter (detection) is 173° . This cuvette is resistant not only to aromatic and aliphatic solvents but it is also resistant to acids.

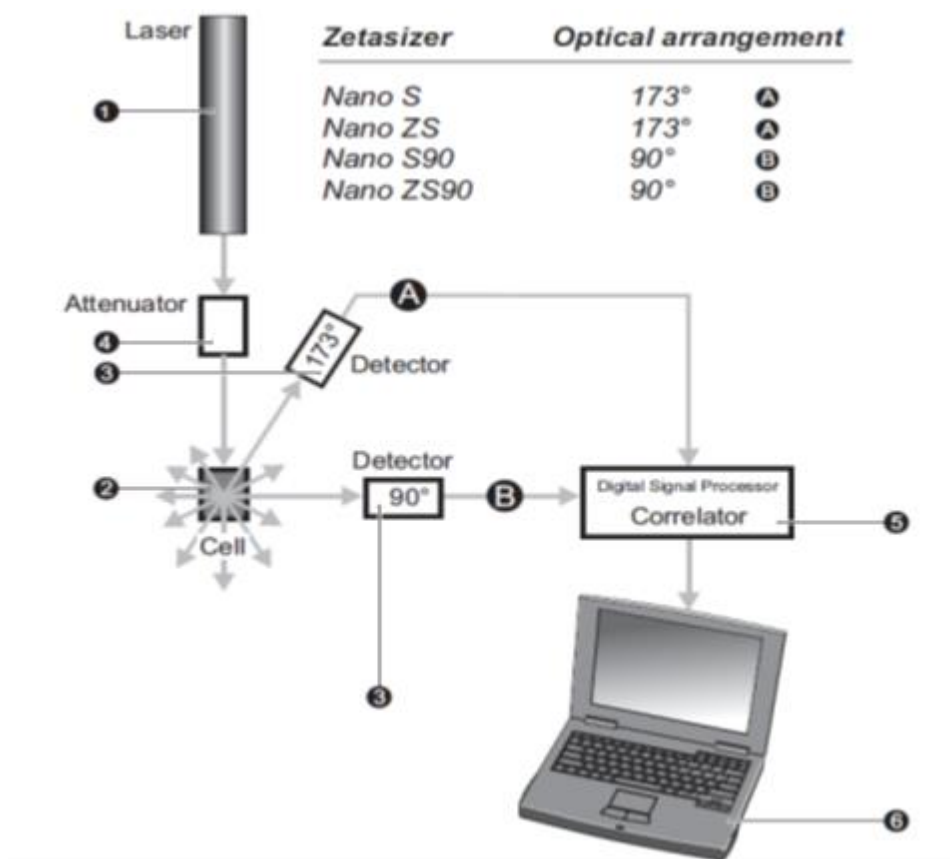


Figure 2.1.2 (a) illustrates the complete set up of a nano zetasizer, which includes a laser, an attenuator, and two sets of detectors, a digital correlator, and a computer. Reference: Zetasizer Nano Series User Manual MAN 0317 Issue 1.1 Feb.2004. chapter 13. page 13.6

To understand in detail about the working of a Nano zetasizer refer to figure 2.1.2 (a)

For measuring the zeta potential and the electrophoretic mobility:

- (1) Disposable folded capillary cell: this is a disposable cell with electrodes, used to measure zeta potential and electrophoretic mobility of nanoparticles in a solution.
- (2) Dip cell: this is very reliable and easy to use cell, the advantage of this cell is that it avoids cross contamination of samples and gives accurate results. This has palladium electrodes; this cell is resistant to hydrocarbon solvents

(3) High concentration cell: in this type of cell the solution does need to be diluted to get accurate results.

(4) Surface zeta potential cell: it is used to measure the surface zeta potential of various surface like non-metals and polymers.

2.1.2 (B) Optics of DLS nano zetasizer:

When the laser light hits the sample light gets scattered in all direction. These angles are known as back scatter angles and technology that uses these angles to measure the size of the nanoparticles is known as non-invasive back-scatter (NIBS). Let us understand why these angles are chosen. They are chosen to reduce the path length of the laser in the sample. When the path length is reduced, higher concentration of the sample can be measured. Also when the laser hits a particular nanoparticle, it gets scattered by other nanoparticles causing a phenomenon referred as multiple scattering. This can cause errors in results. To reduce multiple scattering back scatter angle of 173° is used. An interesting fact should also be noted here is that there are dust particles and larger aggregates present in the solution when light hits on these particles. It is generally scattered forward. Therefore when back scatters are measured it reduces the effect of dust nanoparticles. The zetasizer also uses movable lens to change the position of focus within a cell, allowing larger concentration of sample to be measured. An angle of 90° is also used to measure the scatter, but it is done rarely only in specific cases.

2.1.2 (C) Digital signal processor (correlator):

The zetasizer records the fluctuation in the intensity of the scattered light. And this is how the instrument calculates the size of the nanoparticles. It is important to know how the entire process occurs. It happens due equipment called as the digital correlator. What a correlator does is that it measures how two signals at time period t are similar to each other. Using this it builds the size of the nanoparticles. The answer to this is that, the nanoparticles are in continuous Brownian motion and the velocity of the nanoparticles varies with the size of the nanoparticles, where in large nanoparticles move slowly and smaller nanoparticles move with a higher velocity. The intensity of fluctuations in the laser are directly proportional to the size of the nanoparticles, lesser the size of the nanoparticles the quicker they move and higher is the intensity of fluctuation of time (for large and small nanoparticles). Once the instrument measures the correlation function, the software present in the DLS nanosizer then uses sophisticated algorithms to calculate the size of the nanoparticles. along with the size of the nanoparticles the computer also displays the number, intensity and the volume distribution.

2.2 UV-Vis-Spectroscopy

UV-Vis-Spectroscopy has been one of the most important tools of analysis in a nanotechnology laboratory. It is also, an important tool for laboratories working in organic, inorganic chemistry and nano-biotechnology. A spectrophotometer is an essential aid in both research and routine analysis as it is easy to handle, and using several properties can be analysed and understood. The shape, size and the concentration of nanoparticles in a solution can be calculated using a spectrophotometer.

Modern spectrophotometers are quick, accurate and more reliable than their older versions, making the whole process less time consuming and more independent of the skills and knowledge of the operator. However, to use the instrument to its fullest merit and user must know how to operate a UV-Vis-spectrophotometer which basically works on the fundamental

laws of physics. The next few pages shall be dedicated in understanding the design and working of a typical UV-Vis-spectrophotometer, in this process we will also look at the important processes that underline its efficient working.

2.2.1 Electromagnetic spectrum:

In an environment, we are constantly exposed to naturally occurring electromagnetic radiations. Some of them are detected by our senses. Such as the sun's heat is recognized by the body as warmth, while the eyes can see different objects of the light it reflects. But the entire electromagnetic spectrum has wavelengths these cannot be detected by the eyes, and what the eyes can see is very small part of the entire spectrum. If we look at a rainbow it has two ends. At one end where wavelength is increasing it is red and at the wavelength is decreasing it is violet. Red consists of microwaves and radio waves, as the wavelength increases. The other direction beyond violet is called ultra violet, with progressive decrease in wavelength, from X-rays, gamma rays to cosmic rays.

All electromagnetic rays travel at the speed of light which is 3×10^8 m/s, in vacuum. The wavelength of the electromagnetic wave is assigned by a symbol called lambda (λ) which represents the distance between two consecutive peaks. The number of waves passing through a particular point at time (t) is denoted as the frequency of the wave (ν).

The relationship between the velocity of light, wavelength and the frequency is given by the equation:

$$c = \lambda \nu$$

Using the law of quantum mechanics which when applied to photons

$$E = h \nu$$

Here (E) is the energy of the incident radiation, ν the frequency of the radiation and (h) is the Planck's constant. On combining the two equations we have,

$$E = hc/\lambda$$

The unit that defines the wavelength is (m), for radiations in the visible region the wavelength is defined in terms of nanometer (nm) or Angstrom (Å).

The visible end of the electromagnetic spectrum has radiations with a wavelength between 380 nm to 770 nm and the ultraviolet region has radiation of wavelength between 200 nm to 380 nm.

2.2.2 Beer and Lambert's law of absorbance and concentration:

Lambert's law:

According to the Lambert's law, the amount of light absorbed by a transparent medium is independent of the intensity of the light (provided there are no changes in the medium be it chemical or physical). As a result of the layers of the medium having equal thickness will transmit equal proportion of incident light energy.

The Lambert's law is expressed by the equation:

$$I/I_0 = T$$

Where (I) is the intensity of transmitted light and (I_0) is the intensity of the incident light. T is the transmittance. Expressing the equation in percentage transmittance, we have:

$$\%T = (I/I_0) \times 100$$

Beer's law:

According to Beer's law the absorption of light is directly proportional to concentration and the thickness of the absorbing medium in the light path. The combination of the two is called as the Beer-Lambert's law, which defines the relationship between absorbance (A) and transmittance (T).

$$A = \log (I/I_0) = \log (100/T) = \epsilon c b$$

A– Absorbance

ϵ – Function of wavelength

(b) – path measured in cm

(c) – molar concentration

2.2.3 Surface plasmon resonance

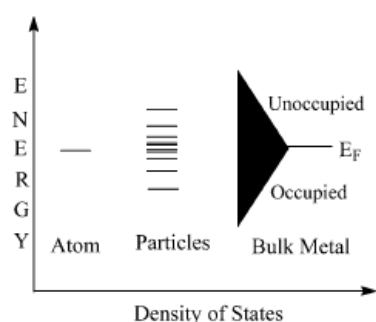


Figure 2. Energy levels in metal particles.

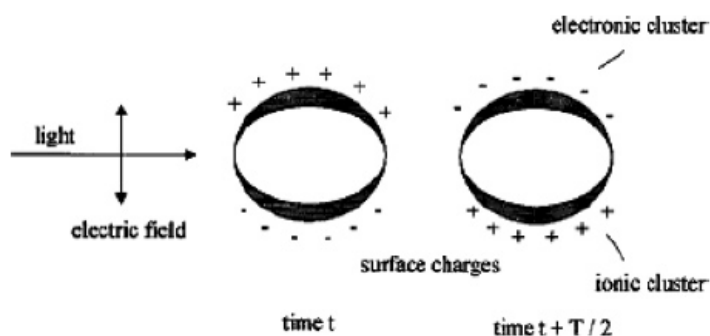


Figure 2.2.3 (a) illustrates the energy levels of metal nanoparticles, and also the image shows the ion clusters around the nanoparticles.

Reference: Basic UV/Visible Spectrophotometry, Biochrom.

When analysing nanoparticles using a UV-Vis-spectroscope, it is important to understand surface plasmon resonance. Light waves contain electric and magnetic component perpendicular to each other. Thus when incoming light waves (electrical component of the light wave) interacts with nanoparticles, there is polarization of the free conduction electrons. The positive charge is immobile, and the negative charge (electron) move under the

influence of electric field. Therefore, there is displacement of negative charge from the positive charge in the presence of electric field which is present in the light wave. This result in charge difference in nanoparticles, creating dipole oscillation of electrons, a collective oscillation of electrons is called as surface plasmon resonance for more detail understanding please refer to figure 2.2.3(a). At this point it should be noted that surface plasmons also exist in bulk metals, but since the size of the bulk material is larger than the light waves.

2.2.4 Working of the Instrument.

The minimum requirements to analyse an absorption spectra of a nanoparticle on a Ultraviolet-Visible-spectroscope are:

1. A radiation sourced that can produce wavelengths in ultra-violet (UV), visible and near infrared (NIR) region.
2. A monochromator which isolates light in single wavelength, and transfers it to a sample compartment.
3. A way to introduce test sample in the sample compartment.
4. A method to detect light intensity.

2.2.4 (A) Source of Light:

The source of the electromagnetic radiation needs to emit radiations during the period of measurement. The intensity of the emitted radiation should be constant and adequate for calculations. Deuterium is used as the source of ultraviolet light as it emits stable radiations in the wavelengths range of 190 nm to 380 nm for long period of time. A quartz envelope is put across the lamp to absorb the heat and also to transfer the shorter wavelength of light. In modern methods the tungsten is coupled with halogen. In recent years xenon lamps have been used as a source of ultraviolet and visible light.

2.2.4 Monochromator:

Monochromator is an instrument that is used to convert a beam of polychromatic light to monochromatic light which is of single wavelength. The essential components of a monochromator are (i) entrance slit; (ii) collimating device; (iii) wavelength dispersing or selecting system; (iv) mirror; (v) slit to exit the light.

There are three ways to achieve monochromatic light are: (i) Filters and (ii) Prisms; (iii) Diffraction grating:

- (i) **Production of monochromatic light using filters:** Filters used for obtaining monochromatic light are usually of glass or gelatine which is the most easily available. Interference filters, made of silica, are used these days on which materials of different refractive indices are deposited to achieve band widths of less than 10 nms. The challenge with using filters is that they cannot provide a continuous spectrum, making it not appropriate for laboratory.
- (i) **Using Prisms:** A single prism or a combination of prisms and mirrors are used to achieve monochromatic light. In this setup one end of the monochromator is the entrance which focuses the beam of light to get a single beam. This beam then hits the mirror which reflects it on the collimator which produces a parallel beam of light that passes through the prism. Once the parallel beam of light passes through the prism and hits on the surface of the condenser, the parallel beam of light becomes a single beam. The mirror guides the single beam of light into the exit slit. The advantages of using mirror, and reflected into the exit slit. The advantages of using a prism monochromator are that a bandwidth of up to 1 nm can be achieved using a prism combination and also the performance is much better. The drawbacks of using a prism monochromator are: (i) the dispersion obtained certain times is non-linear in nature; (ii) The mechanism necessary to provide convenient wavelength control is difficult.

- (ii) **Using diffraction gratings:** A Grating consisting of series of parallel grooves on a reflecting surface that are made by taking a replica of the surface from the original surface. The light interacts with each groove separately, where each groove is considered as a separate mirror. The light also interacts with the light reflected from other grooves and produces interference patterns, by changing the angle of incidence of the beam, and a particular wavelength can be selected.

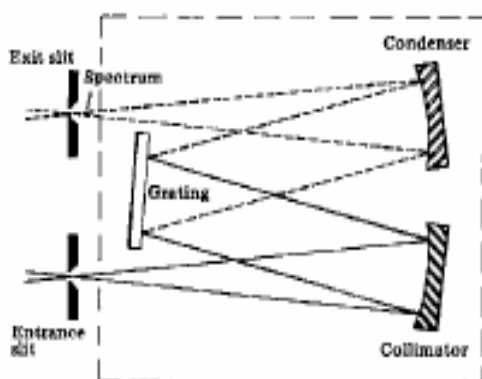


Figure 2.2.4 (B) (a) illustrates the arrangement of condensers, collimators and gratings. Reference: Basic UV/Visible Spectrophotometry, Biochrom. <http://www.biochrom.co.uk/download/72/>

The advantages of using diffraction gratings are: we get better resolution, linear dispersion and continuous band width.

The figure 2.2.4 (B) illustrates a typical diffraction grating monochromator. It works on the principle that as parallel radiations light up a reflection diffraction grating. The reflections from mirror grooves overlap and interact with each other.

If there is in phase interference of reflected waves, this is called as constructive interference, and there is no change in the reflected light. if the interference is out of phase then it is called as destructive interference and the wavelength at which this occurs, these wavelengths will not be propagated.

The relationship which determines the wavelength of light is given by:

$$n \lambda = 2 d \sin\theta$$

Where n is the order, d is the separation between the grating and θ is the angle of incidence of the radiation.

2.2.5 Optical design of the UV-Vis-spectroscope:

2.2.5 (A) Double beam optics:

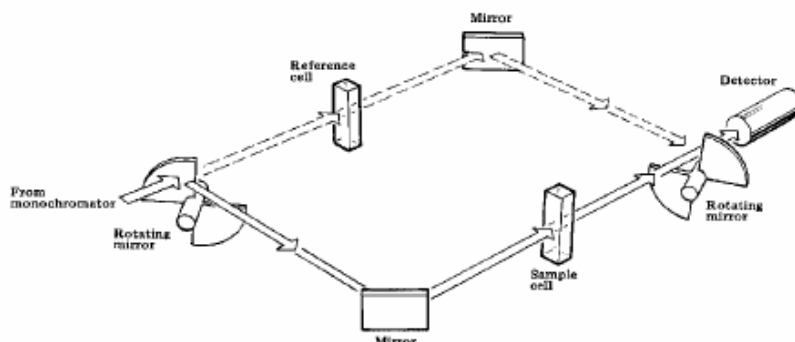


Figure 2.2.5 (A) (a) the diagram shows the double beam optics arrangement. Reference: Basic UV/Visible Spectrophotometry, Biochrom. <http://www.biochrom.co.uk/download/72/>

The above figure 2.2.5 (A) is that of a typical double beam optic system. Double-beam optic system is achieved by having two systems through which light passes. The 1st system is the sample which has the liquid whose absorbance has to be detected, and the 2nd system is called as the reference cell. The advantage of having a double beam system is to give better results. This is because of the decrease in the functions of the instrument that are dependent on the wavelength, which results in improved operating characteristics.

2.2.6 Cuvettes:

Cuvettes are small tubes of circular or square cross section, sealed at one end, made of plastic, glass or fused quartz and designed to hold samples for spectroscopic experiments. All measurements are done on the sample which is in the form of a solution. All instruments are designed such that measurements can be made in a normal sample container called as a cuvette. It is important that the design, construction and material used in the construction of a cuvette should be such that measurements need to be accurate and sample preparation should be easy.

Most of the cuvettes are made up of glass or UV grade silica, and also resistant to the action of solvents. Common cuvettes have a path length of 10 mm, but cuvettes with longer or shorter path length are also available. There are different types of cuvettes like microcells, gas cells, flow cells, and disposable cuvettes.

2.2.6 Detectors in a UV-Vis-spectroscopy:

There are four principle detectors in a UV-Vis-spectroscopy: (i) Photoconductive cell; (ii) Photomultiplier, (iii) Silicon diode; (iv) Diode array. Photomultipliers have the ability to internally amplify the light signal, giving them the sensitivity and wide spectral range. When light strikes the surface of a photomultiplier there is emission of electrons, which are accelerated by a series of dynodes which are maintained at increasing potentials. Finally the potential of the anode is greater than that of the cathode, but it is proportional to the incident radiation. Geometrically there are two types of photomultipliers, side window and end window.

2.2.7 Measuring the signal of a UV-Vis-spectroscopy:

The spectrophotometer provides a signal in the form of spectra which is proportional to the absorption by the sample at a given wavelength. The entire instrument is made of a microprocessor which is the centre for analysing and displaying of spectra. The measuring of the instrument consists of display unit, memory unit, recorder which records all the spectra. There is also a motor drive unit which controls the filter disc motor, grating motor, and cell holder motor. These units control the working of the gratings, cell and the disc. There is also a control unit that switches on and switches off the lamps. Also present here is the analog to digital convertor. At the centre of all this is a central processing unit (CPU) which is a microprocessor.

2.2.8 Sample preparation and analysis:

Sample preparation for analysis on a UV-Vis-spectroscope is not a difficult task, when the sample is a solution of nanoparticles. The solution of nanoparticles is taken and using a dropper it is dropped into the cuvette (glass cuvette or a plastic cuvette) and it is half filled with the solution. The solution is now ready for analysis on the spectroscope.

Before analysing the actual sample, a blank sample is analysed on the UV-Vis-spectroscope. The blank sample is usually distilled water. The parameters like, scanning wavelength and maximum absorbance is set and the sample is run on the spectroscope.

2.2.9 Good operating practices:

Practices that apply in keeping a house clean, same principle apply in keeping a laboratory clean. All the equipment related to the spectroscope should be cleaned regularly, and sample cuvettes should be thoroughly washed with acid followed by wash with distilled water before and after the use. The equipment should be serviced every six months and the software on the instrument should be regularly updated.

2.3 Atomic force microscopy (AFM)

Atomic force microscopy is a measurement technique belonging to group of instruments called the scanning probe microscopy. It is a technique used to analyze, chemical, material and biological surfaces. There are two other imaging techniques that belong to the same category, is scanning probe microscopy (SPM) and the other is scanning tunnelling microscopy (STM). STM was developed before AFM and SPM, it was first invented by Binnig et al in 1982 at IBM research and development centre in Zurich. This amazing invention is one of the most important inventions of modern science and technology, where simple laws of physics and state of the art technology have been integrated to analyze surface at atomic level. Atomic force microscope was later invented by Gerd Binnig,

Christopher Gerber and Calvin Quate, in the year 1985. An important feature of the AFM is that it uses fine tips to measure and analyze surface properties and topography.

Some of the interesting features of the AFM are that it measures samples in x, y, and z direction forming a three dimensional image of the surface. It can be used in both air and water, making it easy to measure biological samples in their natural environment. It can comfortably measure at nanometer and sub nanometer scale, with a scale of 1-10 nm. It can also measure surfaces that are not good conductors of electricity; AFM also finds its application in measuring and realizing surface and inter-surface properties like mechanical, magnetic, electrical, thermal, optical and chemical properties. Due to its complexity, AFM finds much diverse applications than SPM and STM. AFM is applied in the delivery of drugs to their specific sight in cells. AFM can be used to analyze the surface of proteins and nucleic acids like DNA. It has been extensively used to study cell surfaces and structures. In nanotechnology, AFM is applied to study the surfaces of nanoparticles, particularly their shape and crystal structure, thickness and height.

Atomic force microscopy works in a way that a sharp tip is mounted on a reflective surface called the cantilever, which scans the surface. A laser is attached to the cantilever and every time the cantilever scans a new surface, there is a change in topography which leads to the spot position in the photodiode, in this way a three dimensional image of the surface is build. Based on the above principle there are four modes in which AFM operates.

(1) Tapping mode

(2) Contact mode

(3) Dynamic mode

(4) Non-contact mode

The tip of the AFM is made of either silicon or silicon nitride (Si_3N_4) attached to cantilever having a low spring constant, a force of about 10^{-9} N is maintained on the cantilever, as the

tip interacts with the sample. The repulsive or the attractive force between the sample and the cantilever, and the tip deflection is recorded and then converted into analogue of the image is made.

The force is maintained constant by measuring the force with a lever sensor and a feedback control circuit (FCU) to control the position of the piezoelectric ceramic. The movement of the cantilever is generated by piezoelectric ceramic which move the cantilever in x and y directions. The importance of a FCU is that it maintains a constant distance between the tip and the sample. Without a FCU the tip would crash into the sample. Also the minute features of the sample cannot be mapped. Using Hooke's law ($F=-kx$ where F is the force and x represents the deflection in the cantilever) constant distance between the tip and the cantilever is made. This is how the force on the tip is calculated, finally a three dimensional image is formed when the scanner moves in the z -direction.

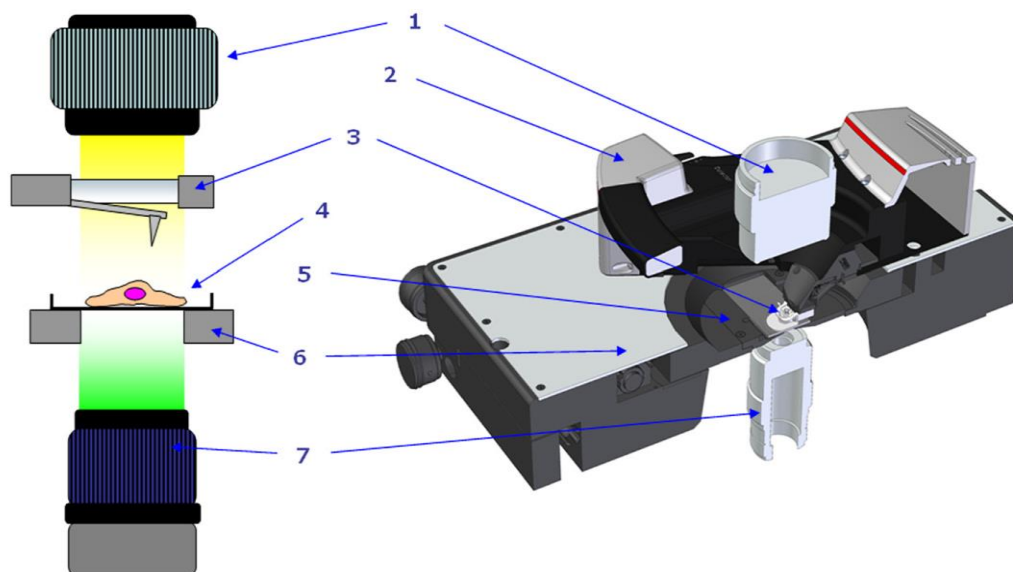


Figure 2.3 (a) (1) Condenser; (2) AFM head; (3) cantilever holder; (4) substrate; (5) sample insert ; (6) piezoelectric ceramic; (7) turret. (Reference: A.Berquand Application Note #138 Combined Optical and Atomic Force Microscopy. Bruker 2012

In a laboratory an AFM as an instrument has a scanner, a computer, control screen and processor, and a monitor that displays the image. The image illustrated in figure 2.3 (a) is that of a typical atomic force microscope, which contains a condenser that perfectly fits the AFM head in its place. The cantilever holder holds the cantilever in place and allows the incident light to pass through it. The sample is laid on a substrate, usually the substrate is glass in case of biological samples, but when objects like DNA and proteins are imaged mica is used as it provides an atomically flat surface which results in high resolution imaging, and better results are obtained. The x-y stage also called as the piezoelectric ceramic moves the sample in x-y direction and allows movement on a larger optical window.

The advantage of the AFM is that it does not require current to operate between the surface of the sample and the tip of the cantilever, and hence it can image insulators, organic substances, and biological molecules.

Let us now look at the different modes of an atomic force microscope.

Contact mode:

This is mode of AFM in which the tip touches the sample and is at distance such that the repulsive forces are greater than tip-sample interaction. The cantilever used is very soft with a force of 0.01 to 1 N/m. The AFM measures the repulsive forces between tip and the sample. When the AFM scans over the sample the tip remains in close contact with the sample. One of the main disadvantages with this technique is that, sometimes due to high lateral forces the tip tends to get dragged across the sample giving a false image.

Tapping mode of the AFM:

This is the mode of the AFM in which the tip does not come in contact with the surface, but it oscillates as it touches the sample surface, collecting vital data as it scans the surface. The cantilever scans the surface with a resonant frequency and a force of approximately 30 N/m.

Tapping or Intermittent contact mode of AFM:

This is a mode of the AFM achieved by oscillating the cantilever at its resonant frequency, but with significantly high amplitude of 10-50 nm. In this mode the cantilever touches the surface only for short periods of time and operates in the repulsive force region. The advantage of this technique is that the damage done to the sample is minimum and this is advantageous with fragile samples. This technique is particularly important when dealing with soft and delicate surfaces. In this technique the amplitude of the cantilever remains nearly constant throughout.

Non-contact mode:

In this mode of the AFM, the cantilever oscillates above the sample and the distance between the sample and the tip is such that there is attraction between the two and the attractive force is Van Der Waals force of attraction. The amplitude of oscillation is low ~ 5nm. In a non-contact AFM the force is measured by taking into account the amplitude of the oscillating cantilever and the signal driving it. The distance between the surface of the sample and the tip of the cantilever is about 10Å. At this distance, the image of the surface is built by the changes in the electrostatic, magnetic and capillary forces.

Let us understand in detail the forces that play a critical role between the tip and surface. When the tip scans the surface, there is potential energy (V_{ts}) between the two: The force produced by this interaction has a z-component. The z component is the distance between the plane that connects the centre of atoms and the atom closest to the tip of the AFM , given by:

$$F_{ts} = -\partial V_{ts} / \partial z \quad (1) \text{ (S. Morita 2002)}$$

F_{ts} is a critical parameter because it is the one that forms the imaging signal. There are also other contributing parameters (electrostatic, magnetic, and van der waals force) which play a

vital role in image topography. Chemical forces are an example of short range forces, and meniscus forces also play a vital role in image formation.

The Van Der Wals potential is given:

$$V_{VDW} = - A_H R / 6z \quad (2) \quad (\text{S.Morit 2002})$$

In the above equation A_H is the Hamaker's constant, which varies from material to material, and depends on the atomic polarizability and density, R is the radius of etched tip. When there is electrostatic potential difference between the tip and the surface of the specimen, it needs to be calculated and accounted for, the equation for the $F_{\text{electrostatic}}$ is given by:

$$F_{\text{electrostatic}}(z) = - \pi \epsilon_0 R U^2 / z \quad (3) \quad (\text{S.Morita 2002})$$

In the above equation R is the radius of the tip and U is the electrostatic potential difference. There are other chemical forces, whose account is given by the Morse equation and Leonard Jones equation:

$$V_{\text{Morse}} = - E_{\text{bond}} [2e^{-\kappa(z-\sigma)} - e^{-2\kappa(z-\sigma)}] \quad (4) \quad (\text{S.Morita 2002})$$

$$V_{\text{Leonard-Jones}} = -E_{\text{bond}} (2 z^6/\sigma^6 - z^{12}/\sigma^{12}) \quad (5) \quad (\text{S.Morita 2002})$$

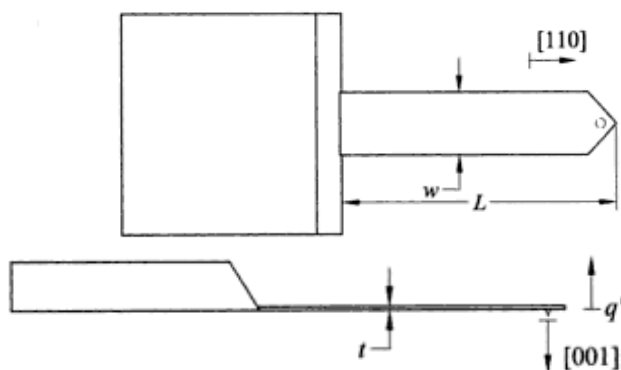
$$E_r = - \alpha/r^6 + \beta/r^{12} \quad (6) \quad (\text{S.Morita 2002})$$

$$F_r = -dE_r/dr = -6\alpha/r^7 + 12\beta/r^{13} \quad (7) \quad (\text{S.Morita 2002})$$

These forces describe the chemical bond potential with bond energy, the Morse equation has an additional parameter called as the decay length κ . Morse equation is the qualitative description of the chemical forces. It should be noted that above equations describe the Leonard-Jones force between the atom present on the tip of the cantilever and the atoms

present on the surface of the sample. The result of the interaction between the tip and the sample surface is measured by the deflection of the cantilever, by a laser beam and photo detector.

The cantilever is characterized by spring constant k and a frequency of f_0 . The spring constant of a rectangular cantilever is given by:



$$k = E_Y w t^3 / 4L^3 \text{ (S.Morita 2002)}$$

$$f_0 = 0.162 t / L^2 \sqrt{E_Y / \rho} \text{ (S.Morita 2002)}$$

Here, E_Y is the Young's modulus; ρ is the density and t is the thickness of the tip of the cantilever and w is the width of the tip of the cantilever. There is another important factor that needs to be taken into account called as the quality factor (Q) which takes into account the damping mechanisms that are present in the cantilever. The cantilevers that work in the air, the

Figure 2.3 (b) illustrates the dimensions of the cantilever. Reference: Noncontact Atomic Force Microscopy, Volume 1, (2002) By Morita S, Wiesendanger R, E Meyer E. Nanoscience and Nanotechnology. Springer

Quality factor (Q) is typically hundred and when working in vacuum it is about several hundreds of thousands.

2.3.1 Resolution of an AFM: A typical microscope (other than an AFM) has a measure of resolution in the focal plane of the image. An atomic force microscope has two resolution modes:

- (i) In plane measurement: This type of resolution depends on the geometry of the tip and the cantilever used in the measurement. The sharpness of the probe plays a vital role in the accuracy of the measurement.
- (ii) Direction perpendicular to the surface: the vertical resolution is achieved by taking into account the relative of the tip of the cantilever above the surface. Maximum resolution can be achieved by minimizing the vibrations.

Chapter 3: Material and methods

3.1 Materials required for synthesis of silver nanoprisms:

Silver nitrate (AgNO_3 , 99% pure), Hydrogen peroxide (H_2O_2 , 30% pure), Tri-sodium citrate ($\text{Na}_3\text{C}_6\text{H}_5\text{O}_7$, 99% pure), Polyvinylpyrrolidone ($\text{C}_6\text{H}_9\text{NO}$)_n, deionized water (H_2O), Sodium borohydride (NaBH_4 , 99% pure), 100 ml flask, 50 ml flask, 10 ml volumetric flask, 50 ml centrifuge tubes, magnetic stirrers, magnetic beads (small). TEM grids, Platinum tipped tweezers, mica sheets 3Inch x 1Inch X 0.006Inch.

3.1.1 Materials required for studying the stability of the nanoparticles in media:

DMEM media (Dulbecco's modified eagle medium), RPMI media, Daphnia media, 30 (25ml) test tubes, fume hood, deionized water (H_2O).

Media formulation:

DMEM media (reference: ATCC (American Type Culture Collection))

<http://www.atcc.org/attachments/4890.pdf>

Table 3.1.1 (a)

Sl. No	Chemical required	Concentration (g/litre)
1	Inorganic salts	
	CaCl_2	0.2
	$\text{Fe}(\text{NO}_3)_3 \cdot 9\text{H}_2\text{O}$	0.0001
	MgSO_4	0.097
	KCl	0.400
	NaHCO_3	1.500
	NaCl	6.400

	NaH ₂ PO ₄ ·H ₂ O	0.125
2	Amino acids	
	L-Arginine·HCl	0.084
	L-Cystine·2HCl	0.062
	L-Glutamine	0.584
	Glycine	0.030
	L-Histidine·HCl·H ₂ O	0.042
	L-Isoleucine	0.105
	L-Leucine	0.105
	L-Lysine·HCl	0.146
	L-Methionine	0.030
	L-Phenylalanine	0.066
	L-Serine	0.042
	L-Threonine	0.095
	L-Tryptophan	0.016
	L-Tyrosine·2Na·2H ₂ O	0.103
	L-Valine	0.094
3	Vitamins	
	Choline Chloride	0.004
	Folic Acid	0.004
	myo-Inositol	0.007
	Nicotinamide	0.004
	D-Pantothenic Acid	0.004
	Pyridoxine·HCl	0.004
	Riboflavin	0.0004

	Thiamine·HC	0.004
4	Other important salts	
	D-glucose	4.5
	Phenol red	0.015
	Sodium pyruvate	0.11

RPMI media formulation:

(Reference: SIGMA ALDRICH; <http://www.sigmaaldrich.com/life-science/cell-culture/learning-center/media-formulations/rpmi-1640.html>)

Table 3.1.1 (b)

Sl. No	Chemical required	Concentration (g/litre)
1	Inorganic salt	
	Calcium Nitrate • 4H ₂ O	0.1
	Magnesium Sulfate (anhydrous)	0.048
	Potassium Chloride	0.4
	Sodium Bicarbonate	2
	Sodium Chloride	6
	Sodium Phosphate Dibasic (anhydrous)	0.8
2	Amino acids	
	L-Alanyl-L-Glutamine	-
	L-Arginine	0.2
	L-Asparagine (anhydrous)	0.05
	L-Aspartic Acid	0.02
	L-Cystine • 2HCl	0.065

L-Glutamic Acid	0.02
L-Glutamine	-
Glycine	0.01
L-Histidine	0.015
Hydroxy-L-Proline	0.02
L-Isoleucine	0.05
L-Leucine	0.05
L-Lysine • HCl	0.04
L-Methionine	0.015
L-Phenylalanine	0.015
L-Proline	0.02
L-Serine	0.03
L-Threonine	0.03
L-Tryptophan	0.005
L-Tyrosine • 2Na • 2H ₂ O	0.02883
3 Vitamins	
D-Biotin	0.0002
Choline Chloride	0.003
Folic Acid	0.001
myo-Inositol	0.035
Niacinamide	0.001
p-Aminobenzoic Acid	0.001
D-Pantothenic Acid	0.00025
Pyridoxine • HCl	0.001
Riboflavin	0.0002
Thiamine • HCl	0.001

	Vitamin B12	0.000005
3	Other important salts	
	D-Glucose	2
	Glutathione	0.001
	Phenol red	0.0053

Daphnia media formulation: (Reference: *Daphnia* Research group (University of Reading) <http://www.biosci.rdg.ac.uk/Research/eb/daphnia.html>

SOP created by Lars-Henrik Heckmann and Richard Connon)

Table 3.1.1 (c)

Sl. No	Chemical name	Concentration (mg/L)
1	Calcium chloride (CaCl ₂ .2H ₂ O)	195.85
2	Magnesium sulphate (MgSO ₄)	82.20
3	Sodium bicarbonate (NaHCO ₃)	64.80
4	Pottasium chloride (KCl)	5.80
5	Sodium selenite (Na ₂ SeO ₃)	0.002

3.2 Methods:

3.2.1 Synthesis of silver nanoprisms

In a 50 ml glass beaker containing a magnetic bead, 25 ml of deionized water was added, the glass beaker is placed on magnetic stirrer. To this solution 2.5 μ l of 0.1mM of AgNO₃ was added, and the solution is vigorously mixed. 1.5ml of 20mM tri sodium citrate was added to the above mixture followed by the addition of 1.5ml of 0.7mM PVP. After 5 minutes of vigorous stirring the add 60 μ l of 30% pure hydrogen peroxide, followed by the addition of 200 μ l of 0.1M sodium borohydride. There was an immediate appearance of pale yellow colour to the solution. The pale yellow disappeared after one minute and the solution turns clear. Stirring was stopped after after the appearance of a clear solution. The solution was left aside for approximately 40 minutes. The solution gradually turned from colourless to sky blue. Monitor the UV-Vis-spectra of the nanoparticles on a spectroscope. The silver nanoparticles are purified using syringe filtration.

3.3 Filtration of nanoparticles using a syringe filter:

A syringe filter is single use filter cartilage, that is attached at the end of syringe and the entire setup is used for filtration of nanoparticles. Commonly syringe filters come in sizes of 0.2 μ m, 0.22 μ m, and 0.45 μ m. The smallest syringe filter had a pore size of 0.02 μ m, refer to image figure 3a.

The following steps were followed to filter nanoparticles using a syringe filter:

- (1) A 0.2 μ m syringe filter was attached to the orifice a 30 ml syringe.
- (2) The filter was rinsed 3 times with deionized water, by filling the syringe with water.
- (3) The solution of silver nanoprisms was sucked in the syringe, and the plunger was pushed and the solution was allowed to pass through the filter. The entire process takes 15 minutes.
- (4) A new filter was used every time a new solution of nanoparticles is filtered.

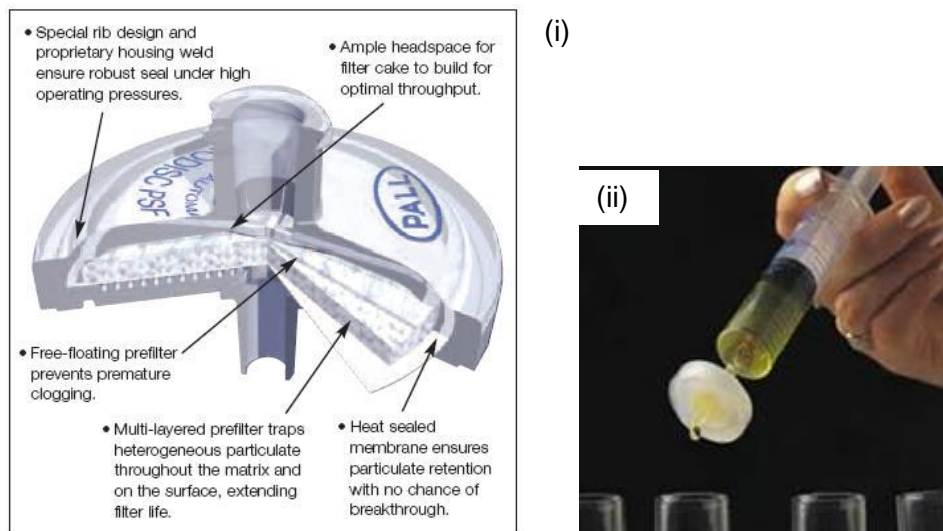


Figure 3a (i) Shows the setup of a syringe filter.

Reference: <http://static.pall.com/images/Laboratory/PSFfig2.jpg>

(ii) Filtration of a solution of nanoparticles through a syringe filter.

Reference: <http://2.imimg.com/data2/GG/BP/MY-2023685/11-250x250.jpg>

3.4 Stability of silver nanoprisms in media:

To study the stability of silver nanoparticles in biological media, three media were chosen, DMEM, RPMI and daphnia media. DMEM and RPMI are media used to culture animal tissue and mammalian cells, daphnia media is a media used to grow *Daphnia magna* which is an important organism in the field of eco toxicology, the effects of nanoparticles are studied considering *Daphnia* (W.X Wang 2010, 2012; P. Rosenkranz 2010; E J Petersen 2009; S B Lovern 2008) as the model organism.

Since these nanoparticles are synthesized with possible application in the field of biotechnology and environmental sciences, it is important to study the toxicity of the nanoparticles to the environment. But, before we can actually study the effects on cells, we have to look at the stability of nanoparticles in biological and eco-toxicological media, to

make sure that the nanoparticles retain original shape, size and surface characteristics. In this case the synthesised nanoparticles are in the shape of a prism, therefore the main aim of this experiment is to study whether the nanoparticles change their shape, and size when they interact with the components of the media (proteins, amino acids, and metal and non-metal salts).

The following steps were taken to study the stability of silver nanoprisms in media:

- (1) A fume hood is chosen for the experiment to avoid contamination by bacteria and other microorganisms DME, RPMI and Daphnia media are taken and poured in a separate container for the experiments.
- (2) Each set had three test tubes, containing media and silver nanoprisms, and deionized water. The changes in the solution are monitored using a UV-Vis-spectroscope, at set time intervals of 0hrs, 24hrs, 48hrs, 72hrs, and 96hrs.

Table 3.3 (a)

Sl. No	Media	Dilution	Amount of media	Amount of silver	Amount of deionized water
1	DMEM	Undiluted	3 ml	3 ml	0 ml
2	DMEM	1:4	1.5 ml	3 ml	1.5 ml
3	DMEM	1:10	0.6 ml	3 ml	2.4 ml
4	RPMI	Undiluted	3 ml	3 ml	0 ml
5	RPMI	1:4	1.5 ml	3 ml	1.5 ml
6	RPMI	1:10	0.6 ml	3 ml	2.4 ml
7	Daphnia media	Undiluted	3 ml	3 ml	0 ml
8	Daphnia media	1:4	1.5 ml	1.5 ml	1.5 ml
9	Daphnia media	1:10	0.6 ml	1.5 ml	2.4 ml

Chapter 4: Results

4.1 UV-Vis-Spectroscopy:

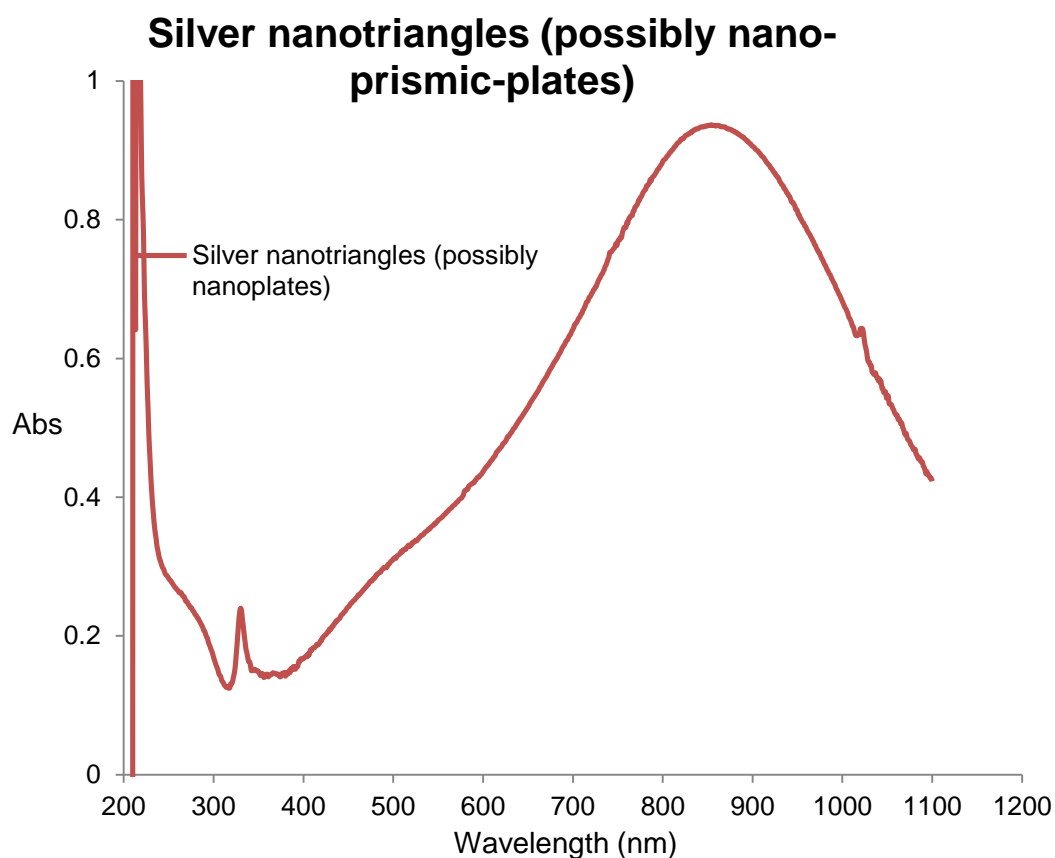
4.1.1 UV-Vis-spectra of nanoprisms.

4.1.2 Variation in UV-Vis-spectra of silver nanoprisms due to the variation in the concentration of H_2O_2 and tri-sodium citrate.

4.1.3 Formation of silver nanoprisms, analysis using UV-Vis-spectra.

4.1.4 Stability of nanoparticles in biological media.

4.1.1 UV-Vis-spectra of silver nanoprisms:



The above graph is a UV-Vis-spectra of silver nanoprisms synthesized using the process of oxidative etching. There are two important peaks to be noted here, 1st is a broad peak at 850 nm, and 2nd peak is the one at 335 nm.

4.1.2 Variation of UV-Vis-spectra due to the variation in the concentration of H_2O_2 and Tri-sodium citrate:

Variation in the concentration of H_2O_2 :

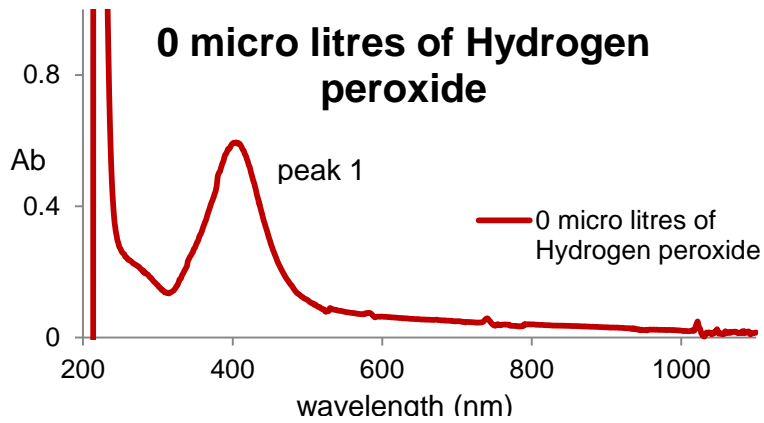


Figure 4.1.2 (a)

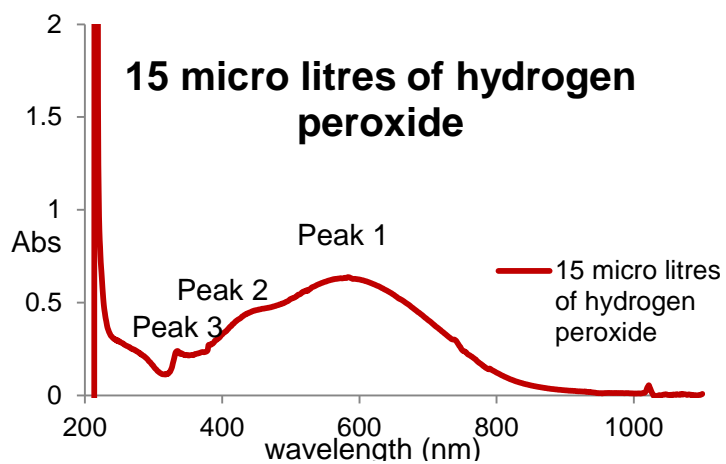


Figure 4.1.2 (b)

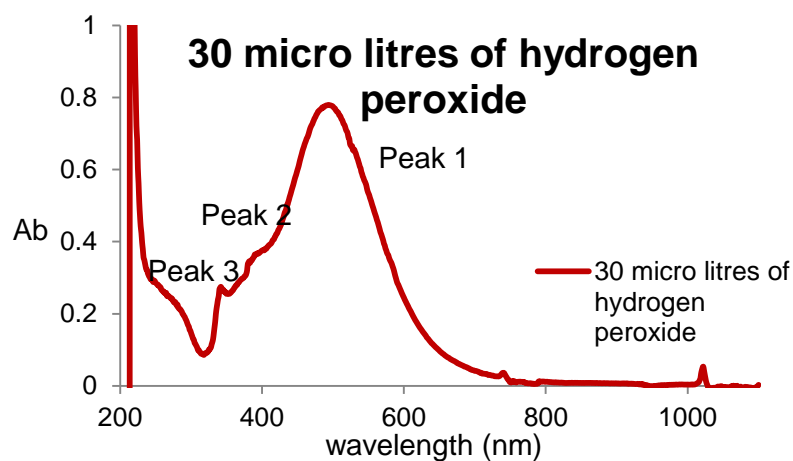


Figure 4.1.3 (c)

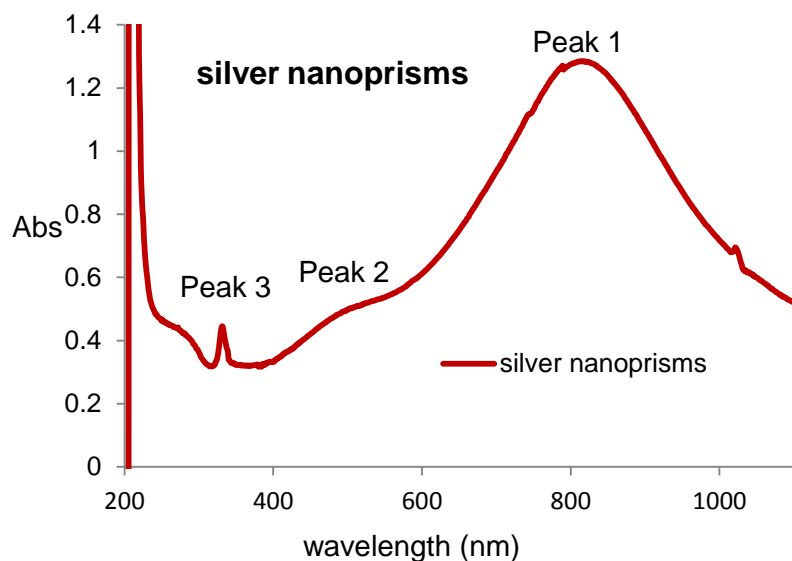


Figure 4.1.2 (d)

Figures 4.1.2 (a) to (d) are the UV-Vis-spectra of silver nanoprisms that are synthesized using the process of oxidative etching using Hydrogen peroxide as the primary etchant. This experiment was conducted to understand the effect hydrogen peroxide on the formation of silver nanoprisms. When the concentration of hydrogen peroxide was $0\mu\text{l}$ the spherical silver nanoparticles were formed, this is evident from the UV-Vis-spectra shown in figure 4.1.2 (a) which has a peak at 400 nm. As the concentration of hydrogen peroxide is increased from $0\mu\text{l}$ to $15\mu\text{l}$ the peak 1 broadens and two more peaks appear, peak 2 at 334 nm characteristic to silver nanoprisms, we cannot still confirm the formation of prisms. When the concentration of hydrogen peroxide is increased to $30\mu\text{l}$ the peak 1 sharpens, but it is between 400 to 600 nm, peak 3 comes closer to 400 nm. At a concentration of $60\mu\text{l}$ peak-1 shifts to 830 nm and peak-2 is between 400 and 600 nm, and peak-3 is at 334 nm, these peaks are characteristic to silver nanoprisms. This experiment shows the impact of hydrogen peroxide on the formation of silver nanoprisms.

Variation in the concentration of Tri-sodium citrate:

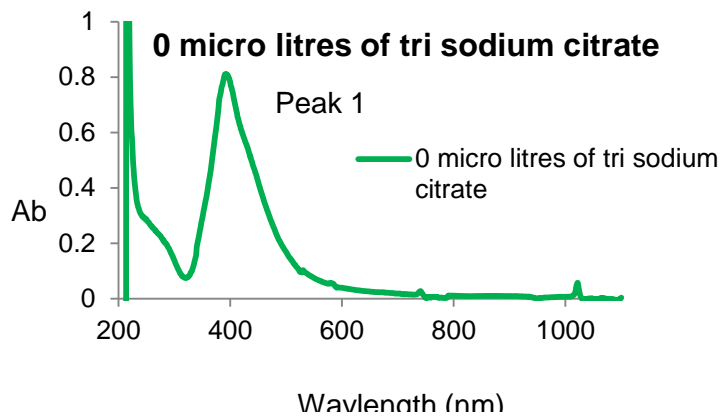


Figure 4.1.2 (d)

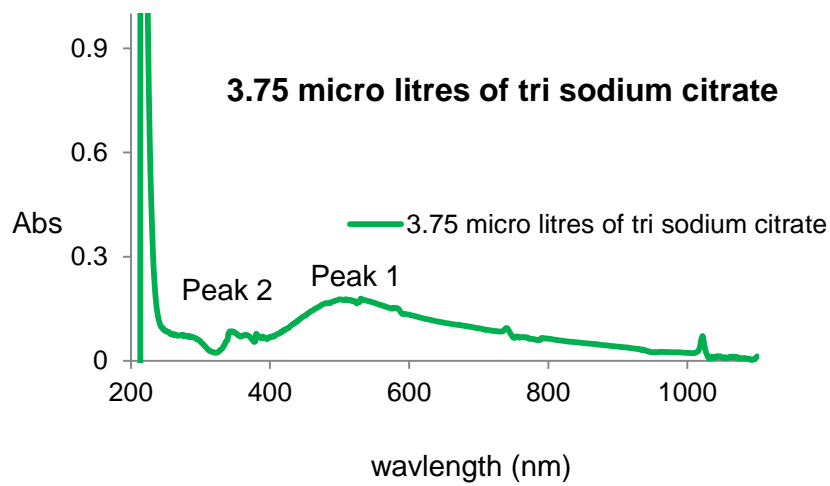


Figure 4.1.2 (e)

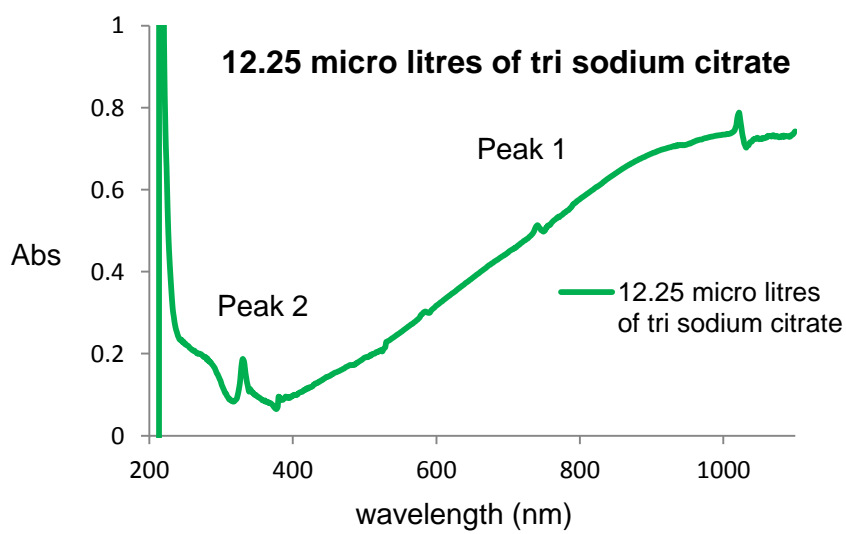
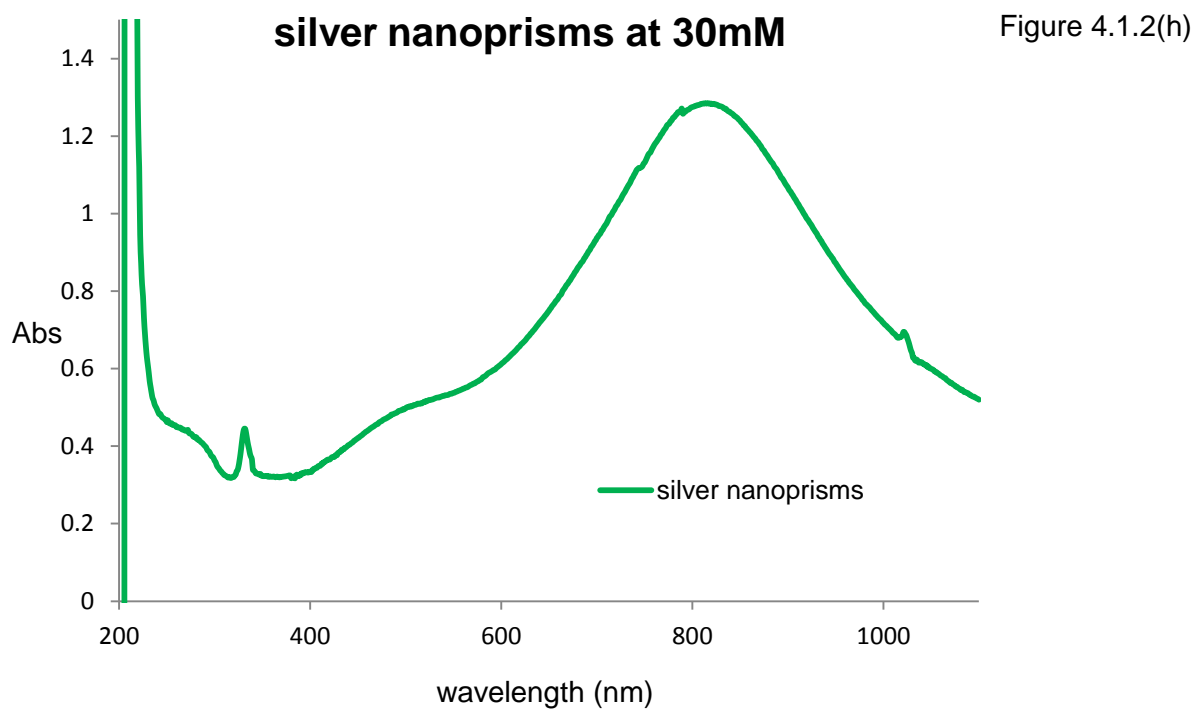
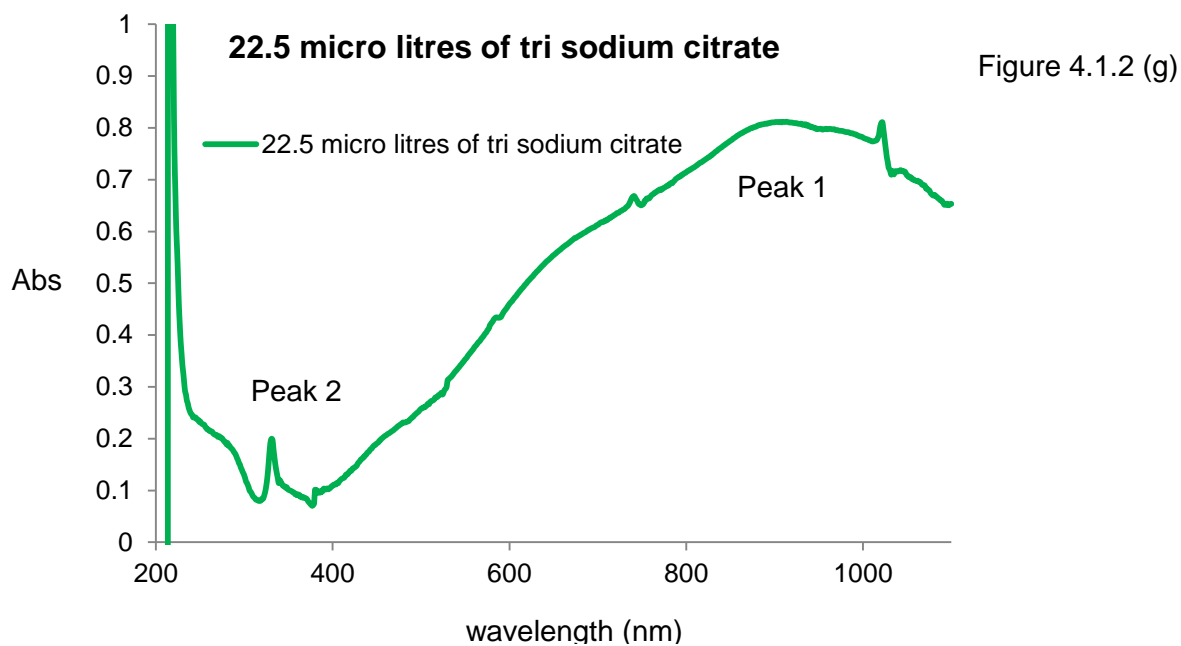


Figure 4.1.2 (f)



The above experiment was conducted to understand the role played by tri-sodium citrate in formation of silver nanoprisms. Figures 4.1.2 (d) to 4.1.2 (g) are graphs showing the UV-Vis-spectra of silver nanoprisms. When concentration of tri-sodium citrate is 0 μl the a peak 1 appears at 400 nm, showing the presence of spherical silver nanoparticles, when the concentration of tri-sodium citrate is 3.75 μl peak 2 appears at 334 nm, and peak 1 broadens

substantially. When the concentration of tri-sodium citrate is 12.25 μ l peak 1 further broadens and goes into near-infrared-red (NIR) region, but the smaller peak 2 remains at 334 nm. We can infer from the above that the nanoparticles are triangular in nature. The broadness of the peak decreases when the concentration of the tri-sodium citrate is increased to 22.5 μ l. When the concentration of the tri-sodium citrate is 30mM, the 2

4.1.3 Formation of silver nanoprisms, monitoring the complete reaction on UV-Vis-spectroscopy:

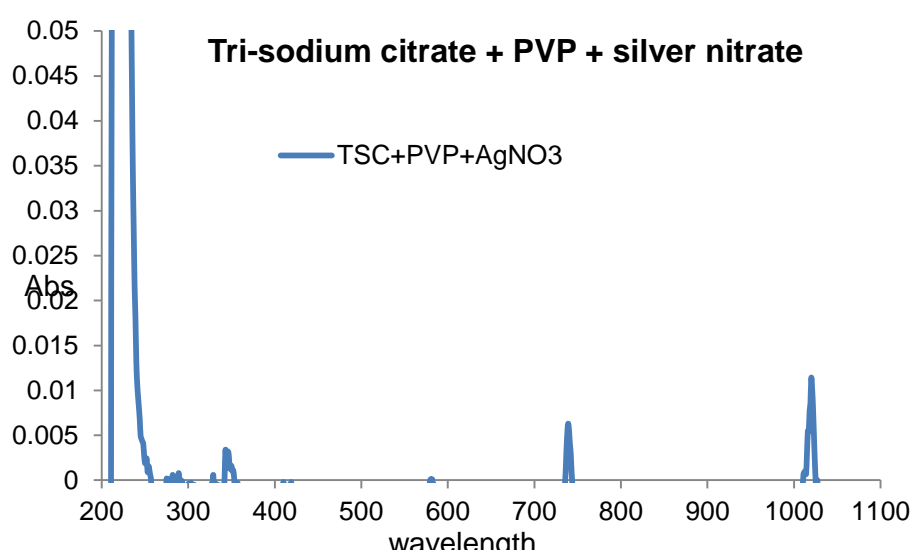


Figure 4.1.3 (a)

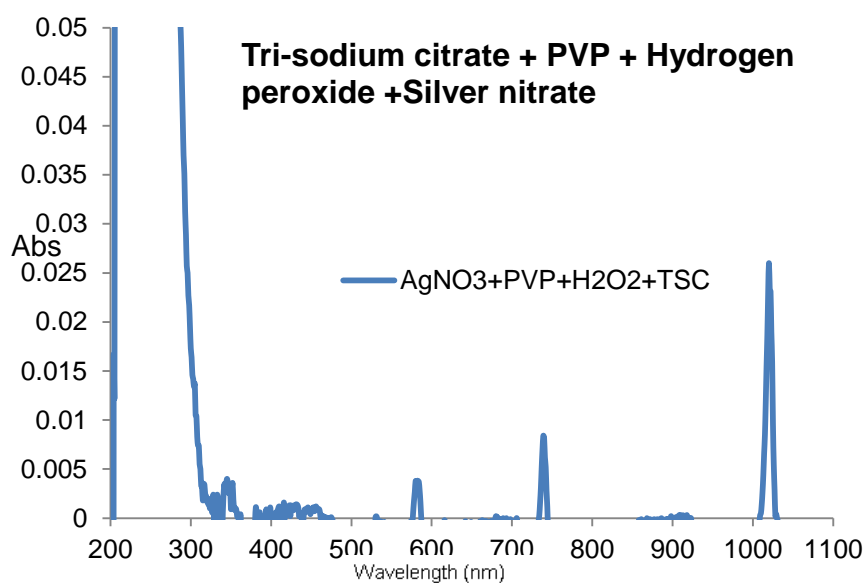


Figure 4.1.3 (b)

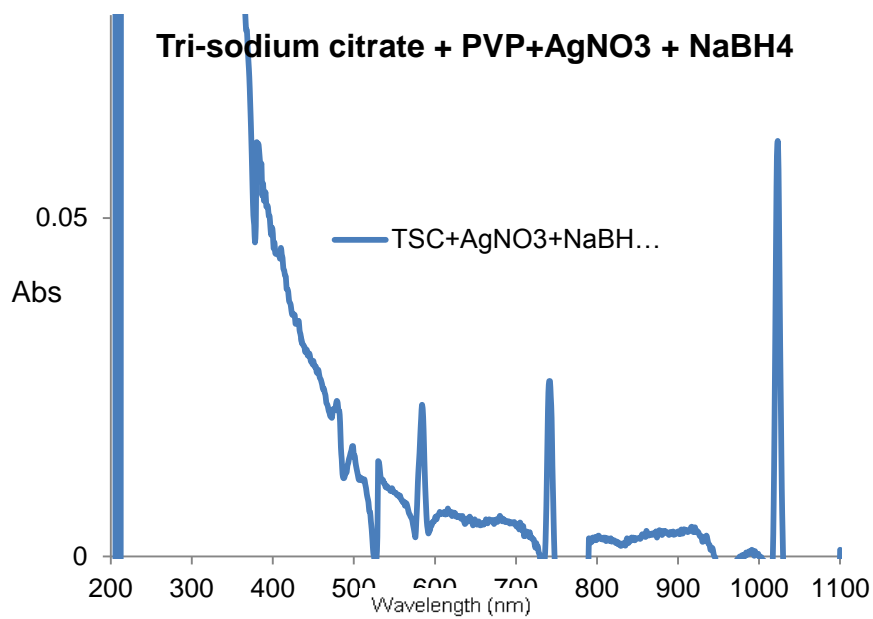


Figure 4.1.3 (c)

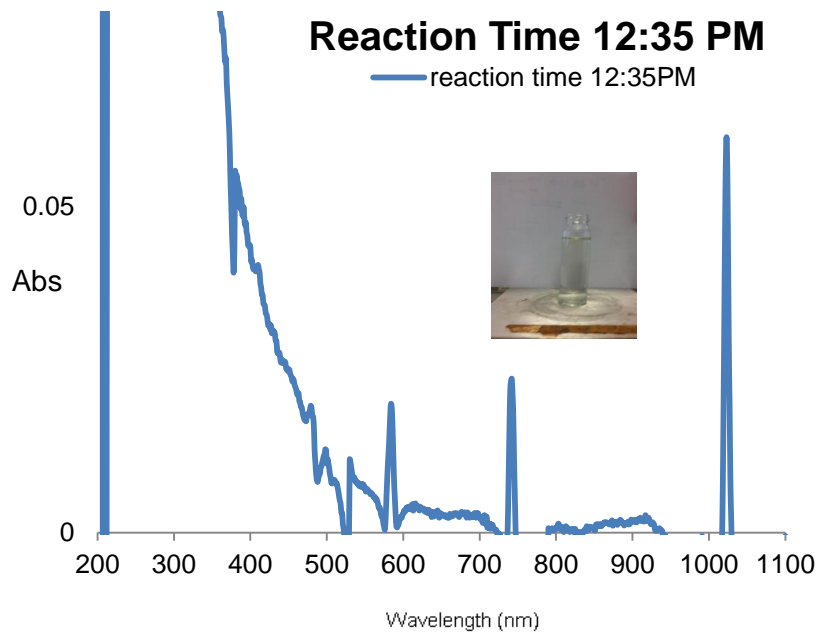


Figure 4.1.3 (d)

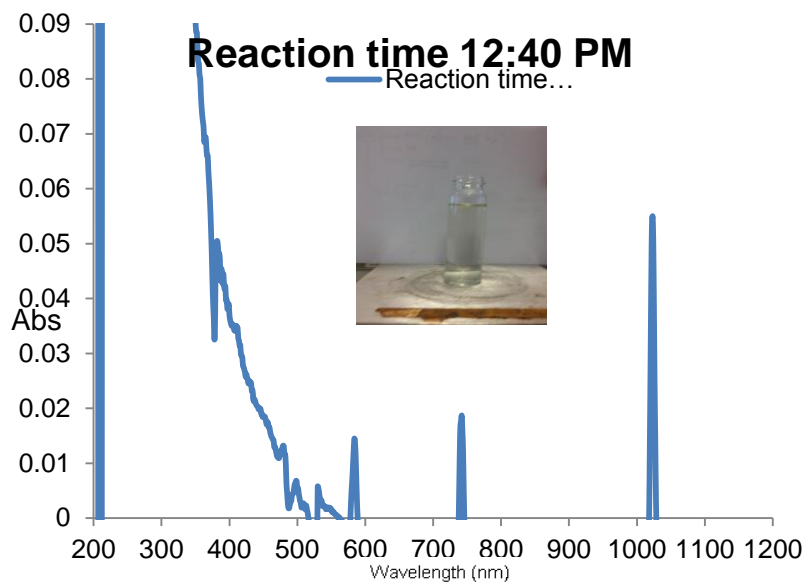


Figure 4.1.3 (e)

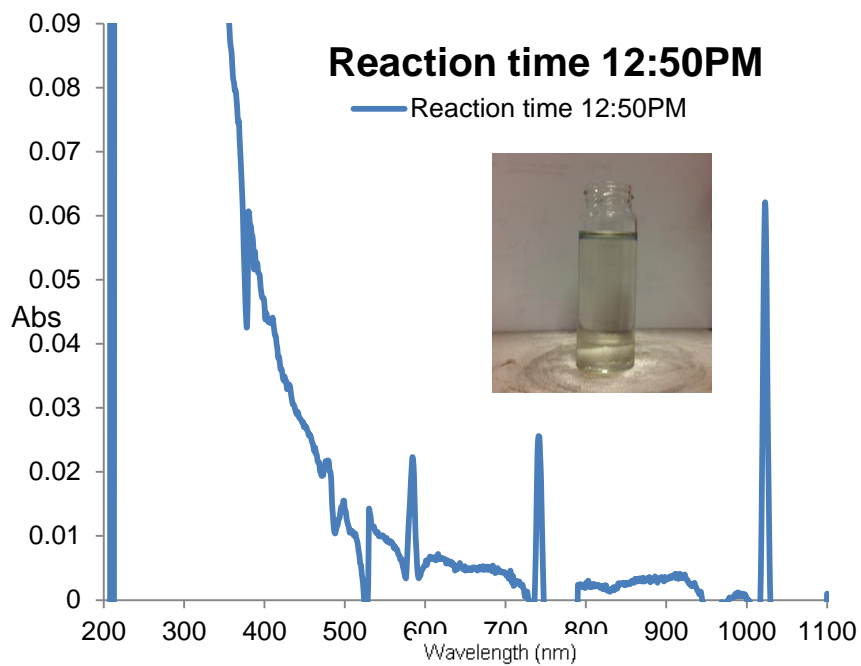


Figure 4.1.3 (f)

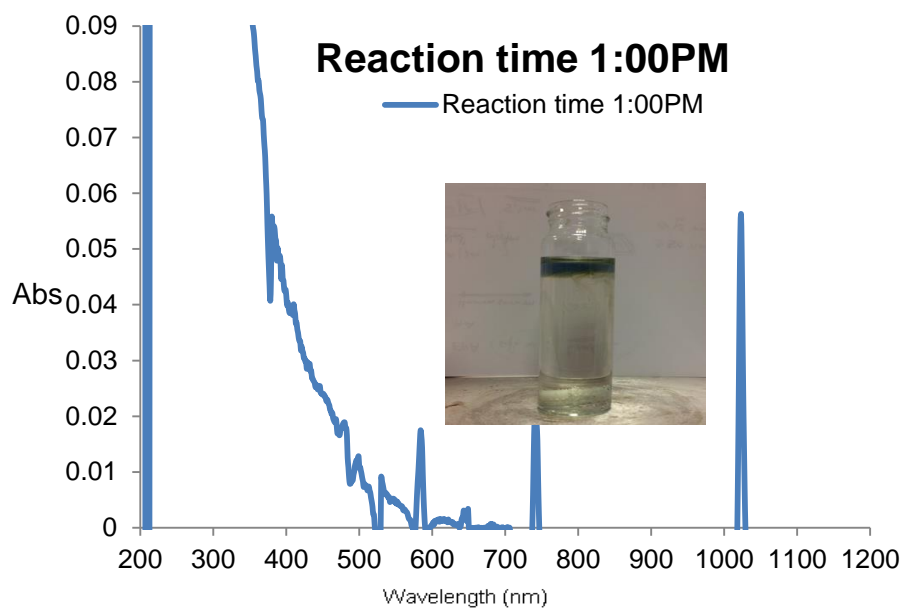


Figure 4.1.3 (g)

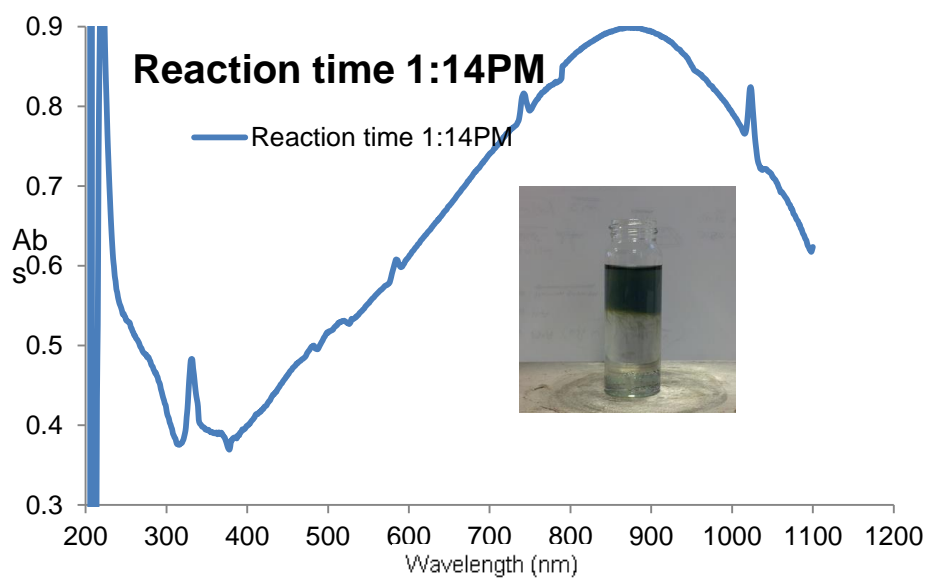


Figure 4.1.3 (h)

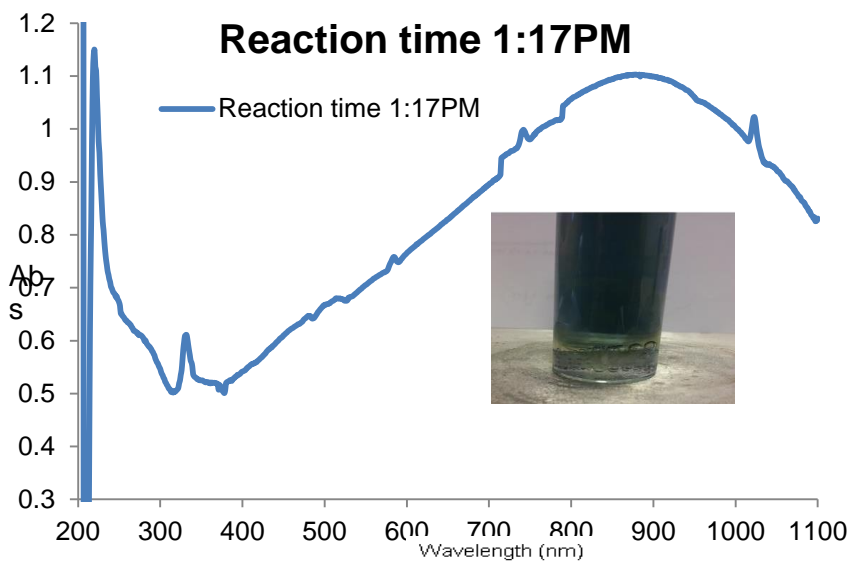


Figure 4.1.3 (i)

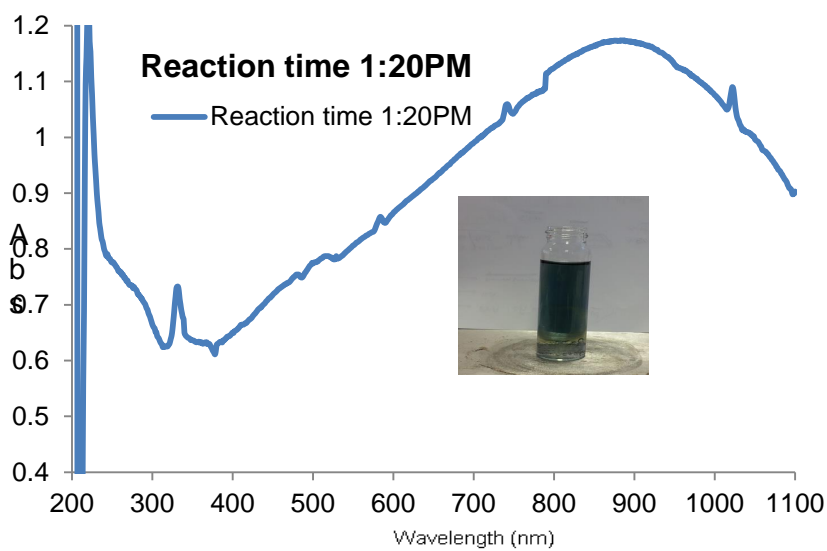


Figure 4.1.3 (j)

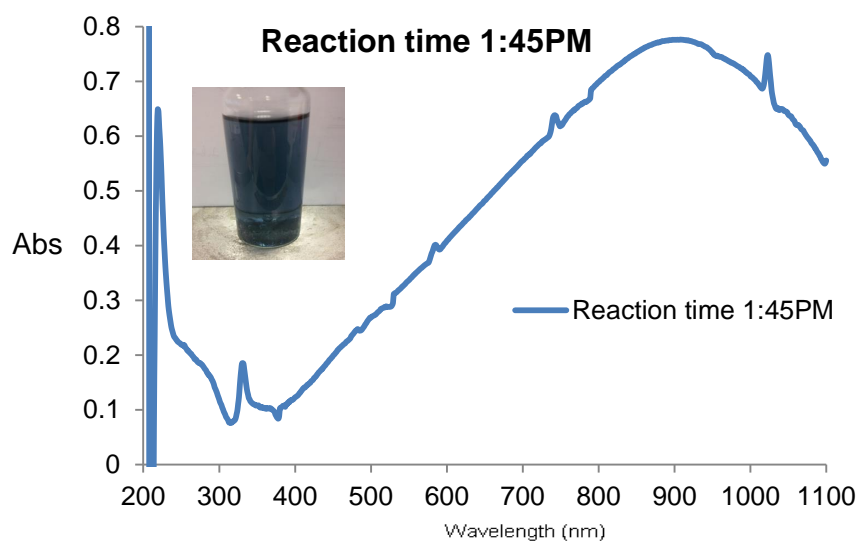


Figure 4.1.3 (k)

The above experiment was conducted to understand, the manner in which silver nanoprimers are formed. The complete reaction takes 1 hour and 10 minutes. The primers formation begins 15 to 20 minutes after the reagents are added; a blue colour layer appears as the nanoparticles are formed.

4.1.4 Monitoring the stability of silver nanoprimers in media using UV-Vis-spectroscopy:

The media chosen for this experiment are:

- (a) DMEM; (b) RPMI; (c) Daphnia media

The nanoparticles are mixed with the media undiluted, diluted in the ratio of 1:4, and a ratio of 1:10. Water is added to the mixture as well. The nanoparticles are monitored over a time period of 72 hours.

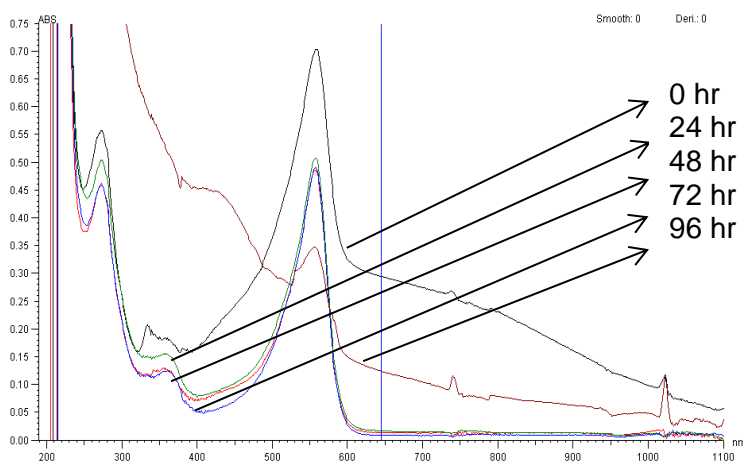


Figure 4.1.4 (a) illustrates the change in absorbance for Silver nanoparticles in DMEM (undiluted) over a period of 96 hours.

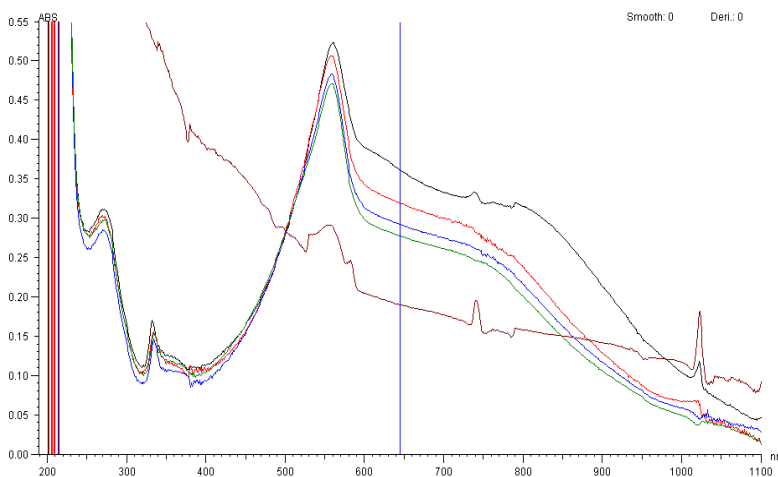


Figure 4.1.4 (b) illustrates the decrease in absorbance for Silver nanoparticles in DMEM (1:4 dilution) over a period of 96 hours.

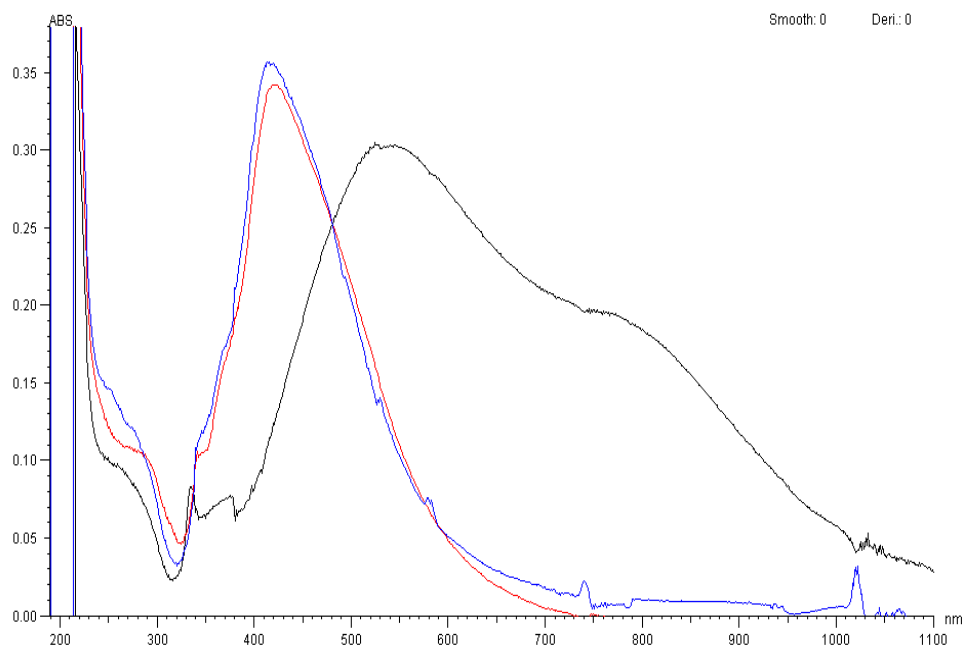


Figure 4.1.4 (c) change in the absorption of silver nanoparticles in Daphnia media (1:4 dilutions) over a time period of 48 hours

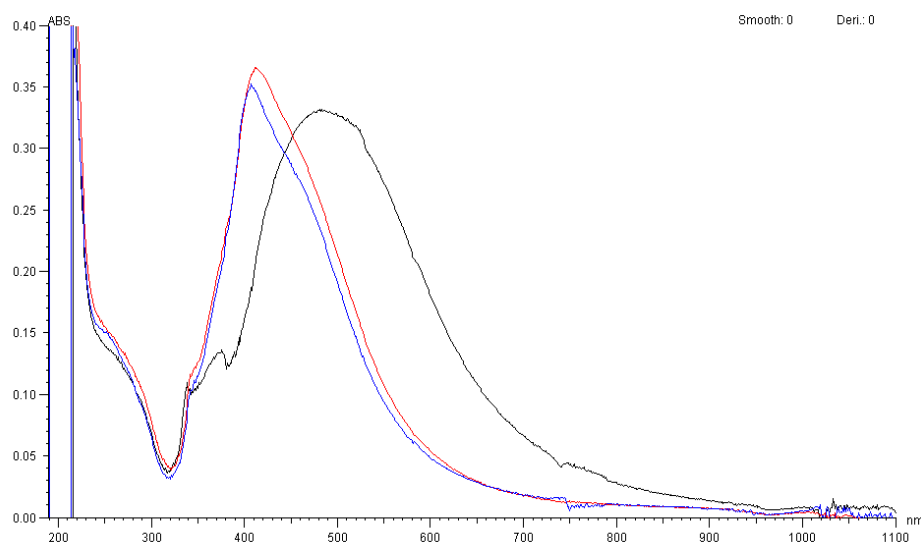


Figure 4.1.4 (d) Show the change in absorbance for silver nanoparticles added to Daphnia media (undiluted)

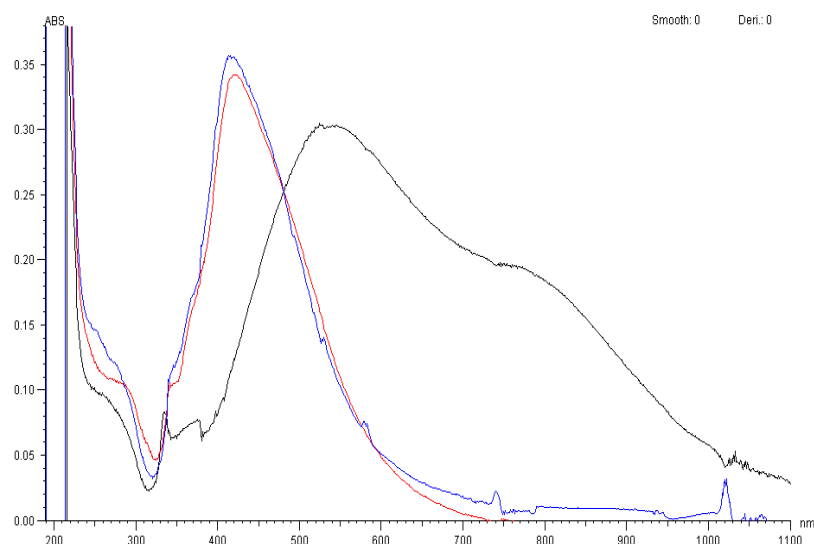


Figure 4.1.4 (e) Change in the absorption of silver nanoparticles in Daphnia media (1:4 dilution) over a time period of 48 hours

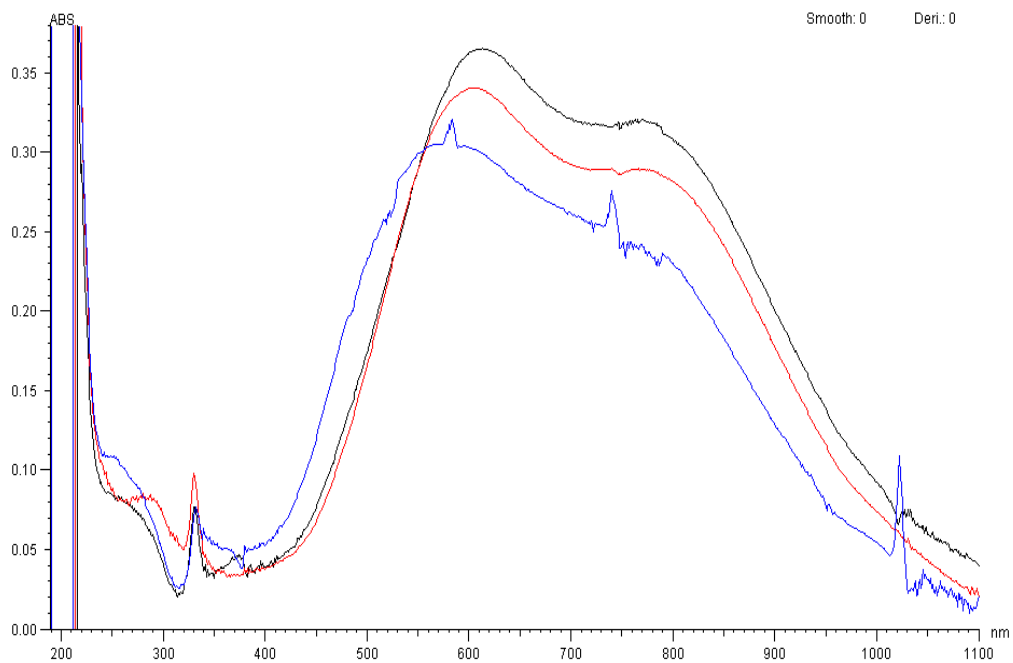


Figure 4.1.4 (f) Change in absorption of silver nanoparticles in Daphnia media (1:10 dilution) over a time period of 48 hours

4.2 DLS Nanosizer

The DLS was used to calculate the size of the nanoparticles, and also it was to monitor the change in the size of the nanoparticles exposed to biological media.

4.2.1 Size of silver nanoprisms

4.2.2 Size of the nanoparticles in biological media

(A) Silver nanoparticles in DMEM (undiluted)

(B) Silver nanoparticles in DMEM (1:4)

(C) Silver nanoparticles in DMEM (1:10)

4.2.2 Stability of silver nanoparticles in media, change in size of the nanoparticles over a time period of 48hrs.

(A) Size distribution of silver nanoprisms in DMEM (undiluted) media.

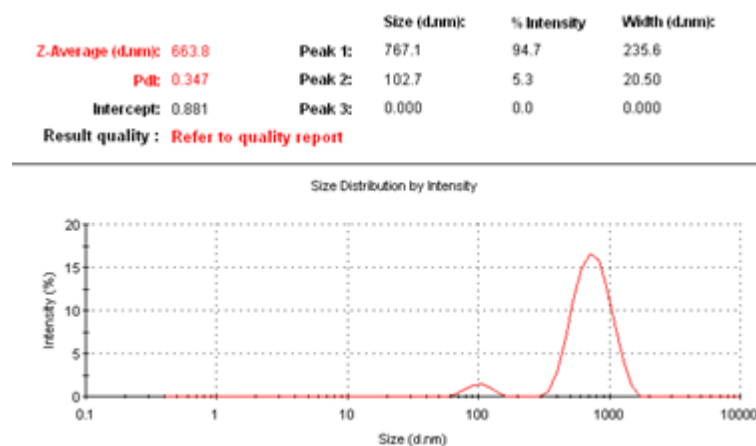


Figure 4.2.2 (a)

Size of the nanoprisms
at Time: 0hrs

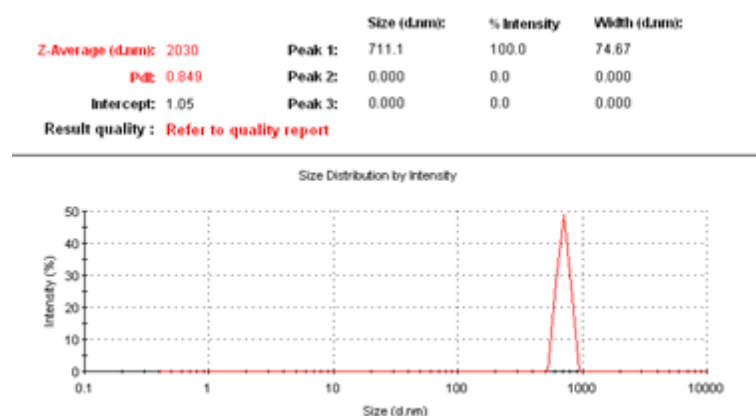


Figure 4.2.2 (b)

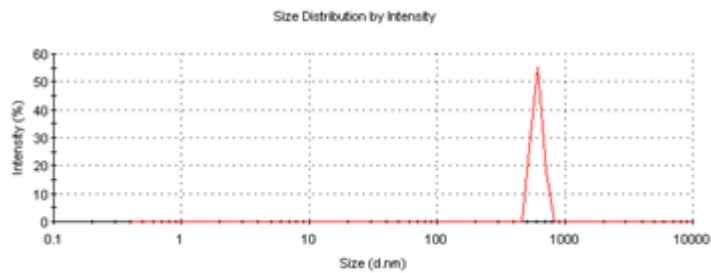
Size of the nanoprisms
at Time: 24hrs

	Size (d.nm):	% Intensity	Width (d.nm):
Z-Average (d.nm): 1942	Peak 1: 610.5	100.0	59.71
PdI: 0.921	Peak 2: 0.000	0.0	0.000
Intercept: 1.09	Peak 3: 0.000	0.0	0.000

Result quality : Refer to quality report

Figure 4.2.2 (c)

Size of the nanoprimers
at Time: 48hrs



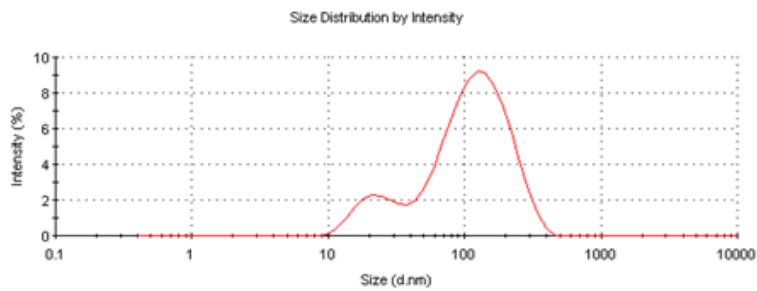
(A) Size distribution of silver nanoprimers in DMEM (1:4 dilution) media

	Size (d.nm):	% Intensity	Width (d.nm):
Z-Average (d.nm): 65.83	Peak 1: 137.5	85.0	70.04
PdI: 0.518	Peak 2: 23.90	15.0	7.713
Intercept: 0.851	Peak 3: 0.000	0.0	0.000

Result quality : Refer to quality report

Figure 4.2.2 (d)

Size of silver nanoprimers
at Time: 0hrs

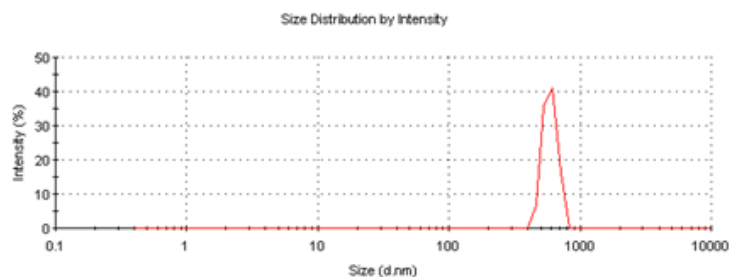


	Size (d.nm):	% Intensity	Width (d.nm):
Z-Average (d.nm): 1188	Peak 1: 590.5	100.0	71.31
PdI: 0.676	Peak 2: 0.000	0.0	0.000
Intercept: 0.959	Peak 3: 0.000	0.0	0.000

Result quality : Refer to quality report

Figure 4.2.2 (e)

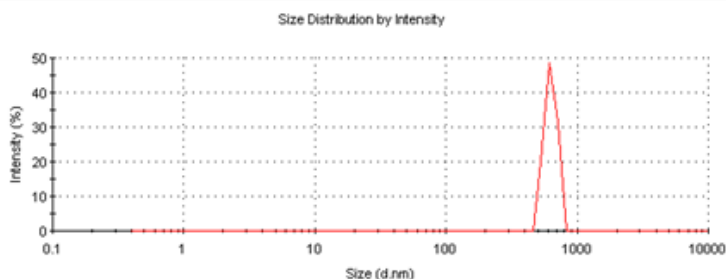
Size of silver nanoprimers
at Time: 24hrs



	Size (d.nm):	% Intensity	Width (d.nm):
Z-Average (d.nm): 1933	Peak 1: 628.8	100.0	64.66
Pdl: 0.976	Peak 2: 0.000	0.0	0.000
Intercept: 1.11	Peak 3: 0.000	0.0	0.000
Result quality : Refer to quality report			

Figure 4.2.2 (f)

Size of the silver nanoprim
at Time: 48 hrs

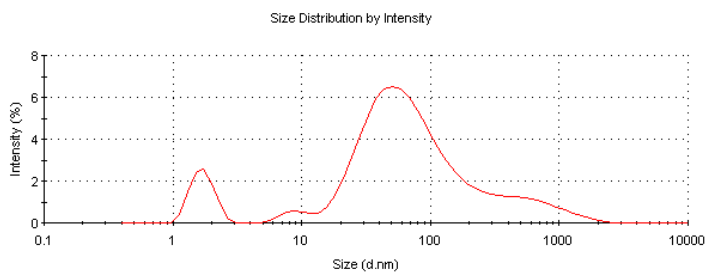


(B) Size distribution of silver nanoprim in DMEM (1:10 dilution) media

	Size (d.nm):	% Intensity	Width (d.nm):
Z-Average (d.nm): 41.05	Peak 1: 153.4	87.8	249.2
Pdl: 0.522	Peak 2: 1.711	9.7	0.3469
Intercept: 0.805	Peak 3: 8.919	2.5	1.809
Result quality : Refer to quality report			

Figure 4.2.2 (g)

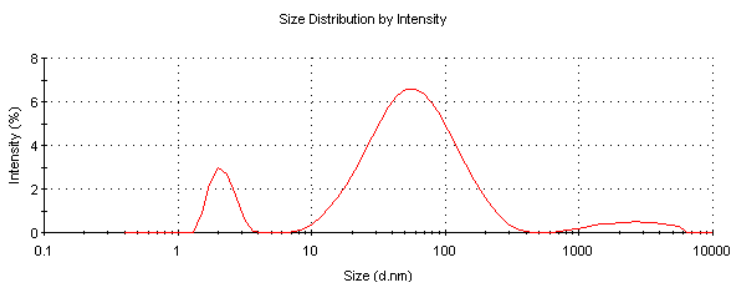
Size of the silver nanoprim
at Time: 0hrs



	Size (d.nm):	% Intensity	Width (d.nm):
Z-Average (d.nm): 34.44	Peak 1: 71.01	83.6	52.92
Pdl: 0.546	Peak 2: 2.161	11.2	0.4324
Intercept: 0.837	Peak 3: 2680	5.2	1336
Result quality : Refer to quality report			

Figure 4.4.2 (h)

Size of the silver nanoprim
at Time: 24hrs



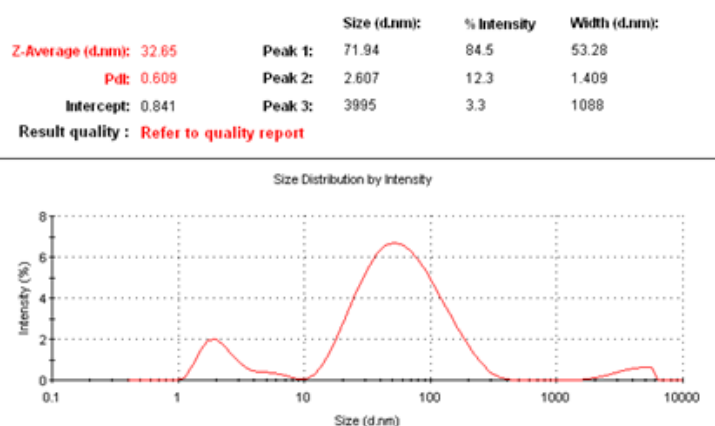


Figure 4.2.2 (i)

Size of silver nanoparticles
at Time: 48hrs

The stability of the nanoparticles in biological media was monitored using UV-Vis-spectroscopy and DLS nanosizer. UV-Vis-spectroscopy was used to see the changes in absorption as the nanoparticles interact with the media. DLS nanosizer was used to monitor the changes in size of the nanoparticles as they interact with the media. The UV-Vis-spectroscopy results illustrated in figure 4.1.4 (a) to 4.1.4 (f) show the loss in absorption in due course of time as the nanoparticles interact with the media. Figure 4.1.4 (a) shows the change in UV-Vis-spectra over a period of 96 hours, with the loss of peaks as the number of hours increase from 24hrs to 48hrs, and so on. The loss in absorption after every 24 hours shows the nanoparticles have changed their shape. The increase in size of the nanoparticles over a period of 48 hours is shown on the DLS Nanosizer. The results are illustrated in figures 4.2.2(a) to 4.2.2 (i) which show the change in the size of the nanoparticles as they are exposed to biological media. Figure 4.2.2 (a) to 4.2.2 (c) illustrates the size distribution of silver nanoparticles in undiluted DMEM media, figure 4.2.2 (d) to 4.2.2 (f) illustrates the size distribution of silver nanoparticles in DMEM media diluted to a concentration of 1:4. Figure 4.2.2 (g) to 4.2.2 (i) illustrates the size distribution of silver nanoparticles in DMEM media diluted to a concentration of 1:10.

4.3 Atomic force microscopy (AFM)

The AFM was used to image the size and shape of the silver nanoparticles. Using this technique we were able to confirm the results of UV-Vis-spectroscopy and DLS. We were also able to determine the width and the height of the nanoparticles using the AFM.

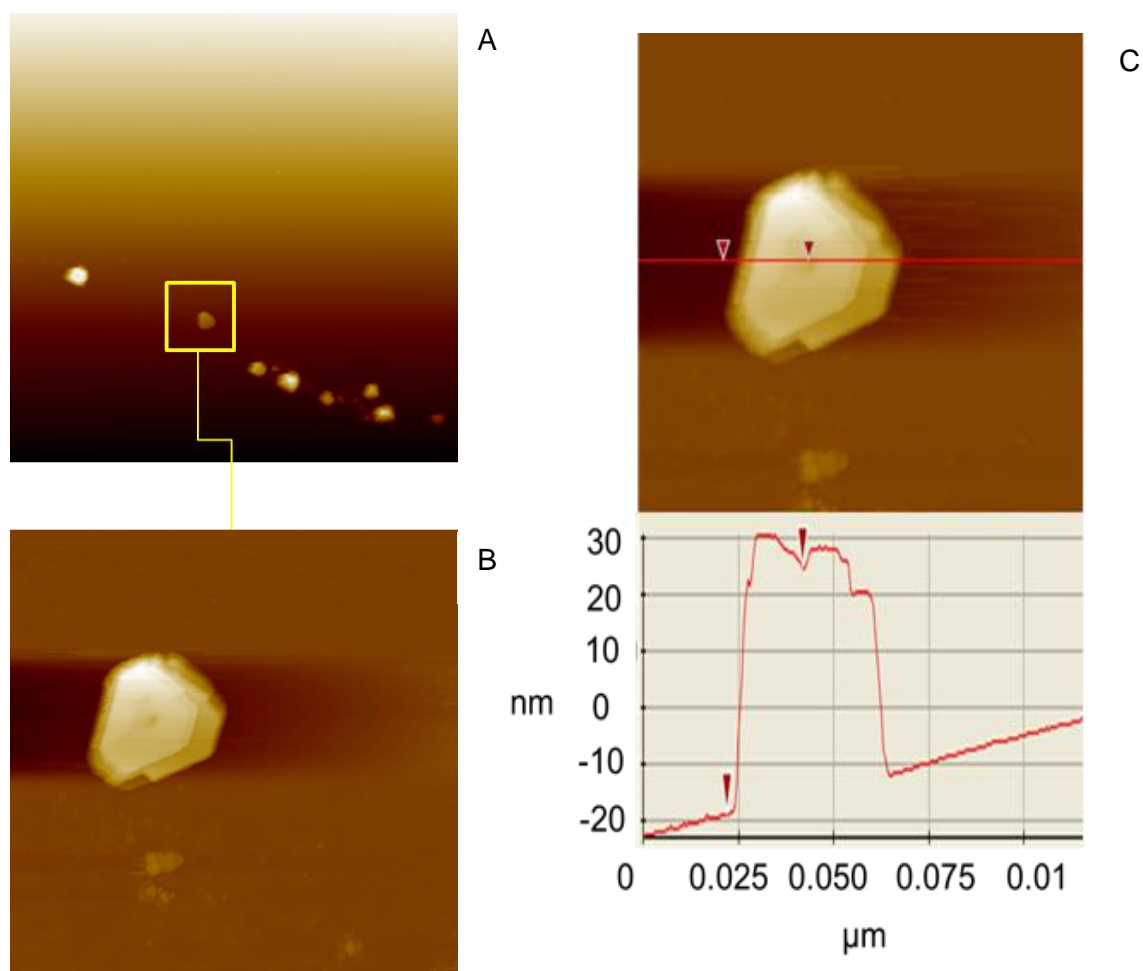
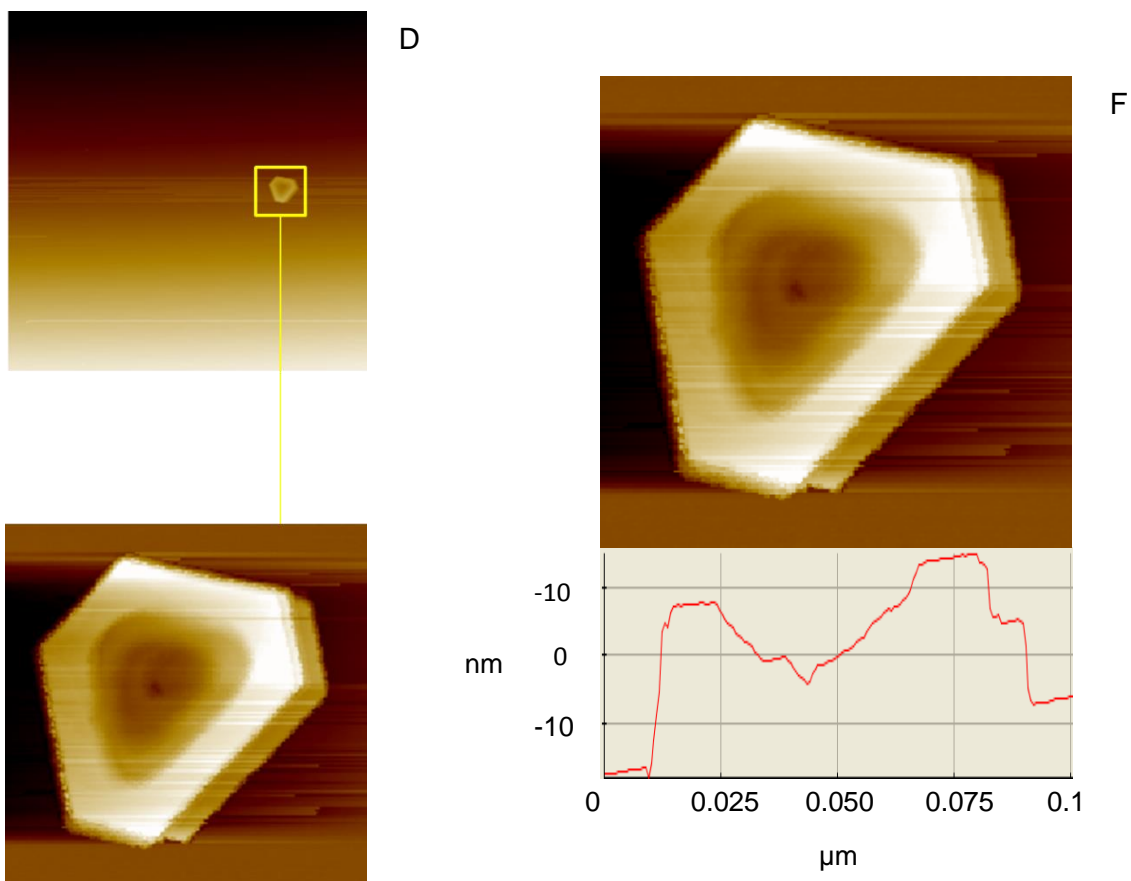


Figure 4.3 (A) shows the image of silver nanoprisms; (B) magnified image of silver nanoprisms show a 'snip' at the three ends of the nanoprisms; (C) this image shows the height and width of the prism.



E

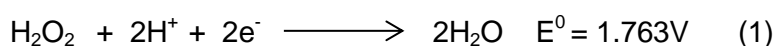


Figure 4.3 (D) shows the image of a snapped silver nanoprism taken on AFM; (E) is a 3D image of a silver nanoprism showing the topographic features of the nanoprism. (E) This image shows the height and width of the nanoparticle; in this case it is 40 nm (size) and a height of approximately 10 nm.

Chapter 5: Discussion

The chemical synthesis of silver nanoparticles is the reduction reaction. In this process the nanoparticles are prepared by reducing an aqueous solution of silver nitrate (AgNO_3) with sodium borohydride in the presence of tri sodium citrate (TSC), polyvinylpyrrolidone (PVP), and hydrogen peroxide (H_2O_2) as the oxidative etchant (Mirkin C. A 2005; Zang.Q 2009, 2010). In this section we will analyse the specific roles of each reagent in the reaction system. The reaction starts by mixing silver nitrate (AgNO_3) with tri sodium citrate, the reagents are mixed using a magnetic stirrer and the reaction is under continuous stirring. Once the tri sodium citrate is added PVP is added to the reaction mixture, along with 60 μl of H_2O_2 . The solution changes from colourless to yellow colour once sodium borohydride is added to the reaction mixture. The solution then quickly changes from light yellow to colourless. It stays colourless for 15 minutes, after which the solution changes from colourless to blue starting from the top of the solution all the way to the bottom of the solution. The UV-Vis-spectra of the solution gradually changes from 400 nm to a shoulder peak at 800 nm, implying the formation silver nanoparticles (evidence: figure 4.1.2(a) to figure 4.1.2 (d)). Let us first understand the role played by hydrogen peroxide in the reaction. It is well known that H_2O_2 is a powerful oxidizing agent. The standard potential for water-peroxide couple is pH dependent.

In acidic solution:



And in alkaline solutions:



Silver has lower potential in both the cases (refer to Equation (1) and (2)) with a potential value of ($E^0 = 0.7996\text{V}$), therefore H_2O_2 can be used as an effective etchant to dissolve metallic silver. Results from the experiment suggest that hydrogen peroxide acts as an

oxidant, and dissolves the silver reduced by sodium borohydride into silver ions. According to (Zang Q 2011) equilibrium should be maintained between the reduction of silver ions by NaBH_4 and dissolution by the metallic silver to silver ions by hydrogen peroxide.

To understand the importance of hydrogen peroxide to the reaction, the concentration of H_2O_2 was varied from 0 μl to 60 μl , the changes were monitored using a UV-Vis-spectroscope (refer to figure 4.1.2 (a) to 4.1.2 (d) in results chapter). When there was no hydrogen peroxide added to the reaction mixture, there was but a sharp peak at 400 nm, indicating the formation of spherical silver nanoparticles, when the concentration of hydrogen peroxide was 15 μl , the UV-Vis-spectra (Chapter 4: Results figure 4.1.2 (b)) shows the appearance of a small peak at 335 nm, and a shoulder peak between 400 to 450 nm, and broad peak at 600 nm, showing the change in shape of the nanoparticles due to the addition of H_2O_2 . At a concentration of 30 μl , there is an appearance of a tall peak at 450 nm, followed by a shoulder peak between 400 nm and 430 nm, and a small but sharp peak at 335 nm, from literature the peak at 335 nm is due to the formation of prisms shape (Mirkin C et al 2009). When the concentration of hydrogen peroxide is 60 μl , silver nanoprisms are formed; a peak at 800 nm and a shoulder peak between 400 nm and 600 nm and a sharp peak at 335 nm are observed. The size of these nanoparticles is measured using a DLS nanosizer, and the average size is found to be 50 nm.

According to Zang Q 2011 the mechanism for the formation of nanoprisms is, that on the addition of NaBH_4 silver ions are partially reduced to silver nanoparticles, which are stabilized by citrate ions and borohydride ions. Once hydrogen peroxide is added to the solution silver nanoparticles are oxidized back to silver ions. This inhibits the growth of the small nanoparticles formed. When there is equilibrium between borohydride ions and NaBH_4 the nanoparticles are small and spherical in shape. Once all the NaBH_4 is exhausted and consumed, there is no protection from the borohydride ions. This allows the production silver nanoparticles of various shapes and structures. Due to the presence of a capping agent citrate and hydrogen peroxide nanoparticles with twinned defects are formed, which favour

the planar growth of nanoparticles. H_2O_2 removes all the unstable nanoparticles leaving all the stable nanoparticles in the solution. The citrate cap the silver nanoparticles by binding at (111) phases of the nanoparticles, therefore the prism shaped nuclei possess highest stability because majority of the surface is capped. Therefore H_2O_2 along with citrate ions functions by promoting the nucleation and growth of silver nanoprisms by removing the less stable structures of silver.

It have also proven the fact that metallic silver instead of silver salts can be used for the preparation of anisotropic structures like silver nanoplates which are the close cousin of the silver nanoprisms. Mirkin and co-workers have also converted spherical silver nanoparticles into triangular nanoplates (Mirkin C.A 2001) using a photo induced method. Y.Xia 2003 thermally converted spherical nanoparticles into triangular nanoplates using citrate as the capping agent.

The advantage of using H_2O_2 for synthesis of silver nanoprisms is that, all the nanoparticles are converted into prism shape irrespective of the shape and size of the nanoparticles.

The advantage of using tri sodium citrate is that, it acts as a shape directing agent and a stabilizer and it has been widely used for the synthesis of Au and Ag nanoparticles of various shapes (Mirkin C.A 2001, 2008). Mirkin and co-workers found that citrate ion serves as a bifunctional reagent in the photochemical conversion of silver nanoparticles to nanoprisms. It converts Ag^1 to Ag^0 and also helps in the formation of prism shape, though the mechanism is not exactly known. They also found out that citrate molecule was the only molecule that could convert silver nanoparticles to silver nanoprisms. Apart from citrate isocitrate was the only other molecule that could convert silver nanoparticles to silver nanoprisms but the yield is very low. Kiline and Xia and co-workers have pointed out that citrate selectively binds to (111) facets and blocks the growth along the vertical axis and promotes the growth along the lateral axis.

PVP is a secondary ligand that is needed for the growth of nanoparticles. According to Mirkin and co-workers nanoparticles of indefinite shape are obtained if the synthesis of silver nanoparticles is done in the absence of PVP. Also, according to observations by (Zang Q 2011) in the absence of PVP, the reaction time decreased from approximately 30 minutes to 3 minutes. PVP molecules slow down the rate of the reaction. The reason why PVP slows down the reaction is because it gets absorbed on the surface of the silver nuclei. The addition of PVP does not allow precise control over the SPR band.

The advantage of using PVP is that it allows the synthesis of monodispersed nanoparticles, and improves the size distribution of nanoparticles. According to experiments conducted by (Zang Q 2011) addition of PVP improved the yield of silver nanoplates and gave a narrow size distribution. In addition Zang et al also found out that similar results were provided by other hydroxyl group containing polymers like ethylene glycol, glycerol, and polyvinyl alcohol. PVP also protects the nanoparticles against excessive oxidation and ripening, thereby controlling the size of the nanoparticles.

NaBH_4 is considered as a very efficient reducing agent to reduce silver and gold ions to atoms. It is widely accepted that NaBH_4 reduces faster at higher concentration than at lower concentrations. But on the contrary (Zang Q 2011) has shown that sodium borohydride reduce the rate of the reaction by binding to the surface of the nanoparticles, the change in nucleation of the nanoparticles affects the size and the aspect ratio of the nanoparticles. reference have also shown that sodium borohydride need not be the only reducing agent to obtain silver nanoplates, they can also be obtained by using reducing agents like, phenyl hydrazine and ascorbic acid.

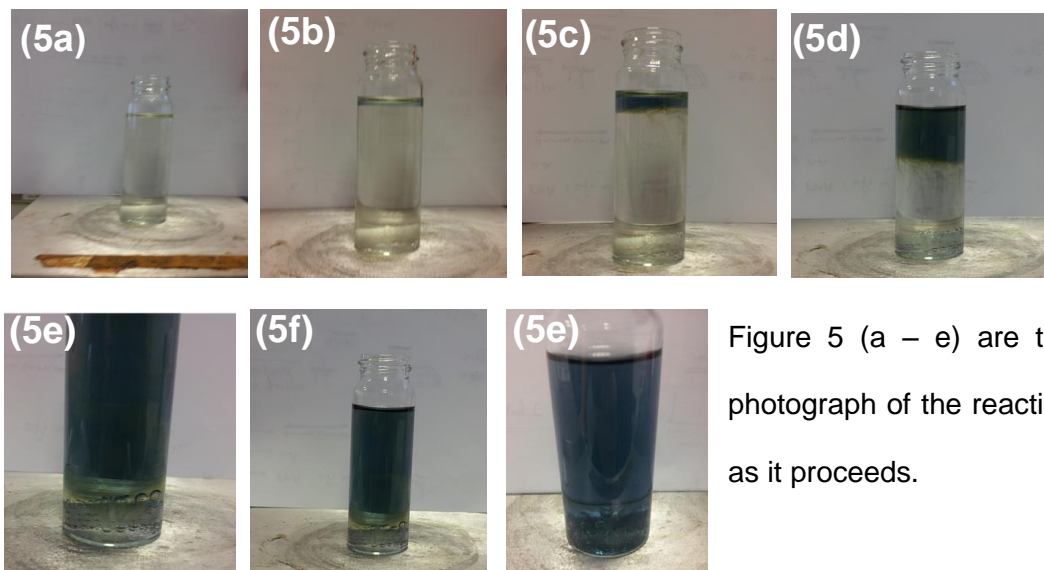


Figure 5 (a – e) are the photograph of the reaction as it proceeds.

Let us understand how the reaction proceeds. The photographs illustrated in figure 5 (a-e) shows how the reaction appears as it proceeds. The total time taken for the reaction to form a complete blue colour is 75 minutes. The reaction begins with a blue colour layer which slowly spreads to the bottom of the test tube. There is appearance of bubbles as the reaction proceeds. The size of the bubbles increases as the reaction approaches its end.



Figure 5(d) shows the appearance of bubbles at the bottom of the reaction vessel as the reaction approaches its end.

The appearance of bubbles can be attributed to release of oxygen and hydrogen in the reaction, as the entire process is oxidative-reductive in nature. A critical observation is that the bubbles are released towards the end of the reaction. Finally the shape, size and the height of the nanoprisms is determined using an atomic force microscope. The images in the results section (refer images in section 4.3 A, B, C, D, E, F) clearly show the triangular shape of the nanoparticle. The nanoprisms have a thickness of approximately 10 to 30 nm and size of 50 nm

Studying the stability of nanoparticles in biological media is very important, as it gives us information on whether the nanoparticles can be used for biological experiments. Mil Tejamaya et al (2011) have conducted vital experiments on the stability of gold and silver nanoparticles in biological and ecotoxicological media. They monitored the change in size of the nanoparticles 21 days in a set of experiments.

In our experiments we used Daphnia media, DMEM media, and RPMI media, for studying the stability of nanoparticles. The Media was added to silver nanoparticles undiluted, with a dilution of 1:4, and 1:10. UV-Vis-spectra and the size of the nanoparticles were monitored at time 0hr, 24hrs, 48hrs, and 72hrs, respectively. Though a strong conclusion cannot be drawn without the availability of TEM images, but from the data that we have we can conclude that silver nanoparticles changed their shape and size considerably in Daphnia media, this is evident from the colour change in the solution after 72hrs, the colour of the solution changed from a distinct blue colour to yellow colour. The UV-Vis-spectra showed a change in the absorption from 800nm to 400nm in a span of 72hrs. When the media was diluted 10 times the colour of the solution does not change even after 72 hrs (this is evident-

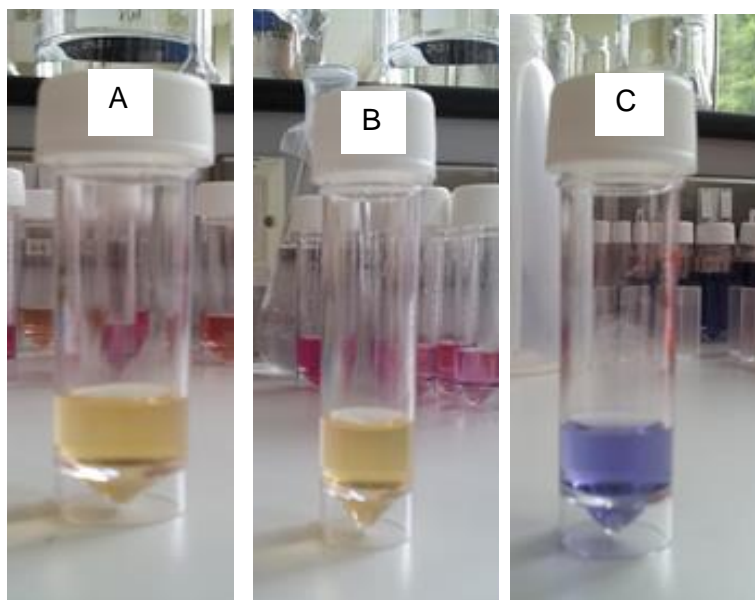


Figure 5(g) Images of AgNPs in Daphnia media for 72 hrs; (A) solution containing silver nanoparticles in Daphnia media (undiluted) (B) solution containing silver nanoparticles in Daphnia media (1:4 dilution) (C) solution containing silver nanoparticles in Daphnia media (1:10 dilution) +AgNPs

From Figure 4.1.4 (f)), there is also not much change in the UV-Vis-spectra. The peak at 800nm remains constant throughout the length of the experiment. The size of the nanoparticle does not change much, this is evident from the DLS Nanosizer results.

In case of DMEM media, the nanoparticles aggregate and change their shape irrespective of the dilution of the media. The solutions change their colour as soon as the media is added to the solution of nanoparticles. The colour changes from blue to red to pink in solution were undiluted DMEM media is mixed with the nanoparticles, in solution were the media dilution is 1:4 and 1:10, the solutions turns from blue to violet and purple.

The size of the nanoparticles changes considerably, with the average size changing from 100 nm to 800 ~1000nm for solution having undiluted DMEM+ silver nanoparticles, 1:4 dilution of silver nanoparticles. Also if you observe figure 4.1.4 (a) the absorbance decreases as we proceed from hour 0 to 72 hours.

Chapter 6: Conclusion

Silver nanoprisms are important to science in technology as they are employed in SERs (surface enhanced Raman spectroscopy) for single molecule detection. In biotechnology silver nanoparticles are used as antibacterial and antimicrobial agent. In nanotoxicology, the toxic effects of silver nanoparticles are tested on different cell lines, to map the pathway taken by these nanoparticles to harm the cell. Most of the studies have been done on spherical nanoparticles, by synthesizing silver nanoprisms, we have opened a gateway to test if the change in shape of the nanoparticle plays a critical role, and does the shape factor increase or decrease the toxicity of silver nanoparticles. Before toxicity tests can be done, it is important to study the stability in terms of their shape and state of aggregation of the nanoparticles in biological and ecotoxicological media, because if the nanoparticles are not stable in the media then it is difficult to conduct testing on live cells.

Hence in this project stability of silver nanoprisms was done on DMEM media and Daphnia media, DMEM is a biological media and Daphnia is an ecotoxicological media. According to the results we can conclude that silver nanoprisms are more stable when the media is diluted with a dilution factor of 1:10, this is quite evident in the UV-Vis-spectra, but to confirm the results it is important to perform TEM (transmission electron microscopy) analysis of the sample. The nanoparticles are more stable in daphnia media than DMEM, the reason being that DMEM is a complex media which consists of proteins, amino acids, and vitamins, which have reactive groups like thiol, amine and carboxyl acid, which react with the nanoparticle and corrode their shape and size, on the other hand Daphnia media has simple composition consisting of metal ions and metal salts (refer to table 3(c)) having a mild effect on the nanoparticle in terms of altering their shape and size. These are initial results and experiments need to be refined and repeated to get concurrent results.

Synthesis of silver nanoprisms is a fairly simple procedure. But better control over the shape of the nanoparticles need to be achieved. We conclude that there are three important peaks

to confirm the formation of silver nanoprisms, a peak at 331 nm called as the out of plane quadrupole (Milestone J.E 2009), the peak at 450 nm is called as in plane quadrupole (Milestone J.E 2009), and the peak at 800 nm is due to dipole resonance (Milestone J.E 2009). In the synthesis of silver nanoprisms, the concentration of hydrogen peroxide (Zang Q 2011) and sodium citrate (Zang Q 2011) is critical for the formation and growth of prisms, though further research needs to be conducted on how exactly these chemicals direct the shape of the nanoparticle.

I would like to conclude by saying that this project makes a successful attempt in synthesizing silver nanoprisms, so that they may be used for biological and environmental applications.

Future work

This project is just the beginning for intense research ahead. The main aim of this project was to synthesize silver nanoparticles and use them for biological and environmental applications, any project in nanotechnology has three phases, synthesis of nanoparticles, characterization of the nanoparticles, and application of the nanoparticles synthesized. Let us now understand the future work that can be done in all the three phases of the project.

Synthesis of silver nanoparticles:

Though we have been able to synthesize nanoparticles of triangular shape, and prism shape, we are yet to get control on the shape of the nanoparticles; the future aim of this project would be to get high yield of silver nanoparticles, with constant edge length. Using inductively coupled plasma mass spectroscopy (ICP-MS), and controlling the chemical kinetics of the reaction, silver nanoparticles should be synthesized. The crystal faces of the nanoparticles should be characterized using computer modelling tools. Using transmission electron microscopy the role played by PVP (surface directing agent), and the capping action of citrate can be studied. This study will be helpful as this will give a better understanding of this not so well understood reaction. Another aspect of this reaction that is unclear is whether the silver nanoparticles are directly converted to silver nanoprism or are there any intermediate structures that are formed before the formation of prism shape. This aspect can be studied by doing TEM analysis of the reaction at various time intervals.

Characterization of silver nanoparticles:

The nanoparticles need to be characterized using an instrument called as NTA (nanoparticle tracker), using this we can understand the mechanism of prisms formation, and also we can estimate the size distribution of the nanoparticles. Since silver nanoparticles are used for single molecule detection, these nanoparticles in future should be also characterized using Raman spectroscopy, to acquire their Raman signals of silver nanoprism. Silver nanoparticles should

also be characterized using X-RD (X-ray diffraction); this technique is useful because it will help identify the crystal structure of the nanoparticles.

Application of silver nanoparticles:

Silver nanoparticles have a wide range of applications both in biological sciences and environmental sciences. In general, silver nanoparticles can be used in photovoltaic, paints and textile industry. Silver nanoparticles can be used to detect biological molecules that are Raman active, silver nanoparticles can also be used as an antibacterial and antimicrobial coating on surfaces. In environmental sciences, silver nanoparticles can be used to study toxicity to various cell lines, in particular to understand how variation in shape plays a critical role in the toxicity of the nanoparticles. In the near future, these nanoparticles synthesized can be exposed to a solution containing only proteins, only amino acids, and only vitamins, this test can be done to understand which of the above three form a corona around the nanoparticle, effect its size and shape, also protein-nanoparticle interaction has been of great interest lately so this experiment would be exciting to perform. Since all nanoparticles are exposed to water at some point in their life cycle, in the next phase of this project silver nanoparticles, should be exposed to different water's, saline water, sea water, sewage water, hard water, and river water. The importance of this study is that using this study we can understand and map the stability of the nanoparticles in terms of their shape and ability to dissolve and produce silver ions which are toxic. The toxicity of the nanoparticles can be studied on various microorganisms, protozoans and multicellular organisms. In Botany, silver nanoparticles can be used to study the uptake of silver nanoparticles by plants; the plants chosen can be aquatic, or terrestrial, a comparative study between nanoparticles of various shapes can be done, to see which nanoparticle is taken up in the highest concentration.

The future looks bright for silver nanoparticles provided they are utilized to their fullest extent.

References

1. G. Aharon; (2007). **Doping nanoparticles into polymers and ceramics using ultrasound radiation.** Ultrasonics Sonochemistry Volume 14, Issue 4, April 2007, Pages 418–430
2. **Basic UV/Visible Spectrophotometry.** www.biochrom.co.uk/download/72; downloaded on 25/11/12
3. Borgohain. K, Singh J.B, Rao R M V, Sripathi T, Mahamuni S; (2000). **Quantum size effects in CuO nanoparticles.** Phys. Rev. B 61, Issue 16 11093–11096;
4. Baker C, Pradhan A, Pakstis L, Pochan Darrin J, Shah S. Ismat; (2005). **Synthesis and antibacterial properties of silver nanoparticles,** Journal of Nanoscience and Nanotechnology, Volume 5, Number 2, pp. 244-249.
5. Berquand A, Lafont F, Hafner M and Petersen M, Schroeder J, Landwher S, and Schwarz U; Hyotyla J, Lim R, Koenig M; (2012) **Application Note #138 Combined Optical and Atomic Force Microscopy.** Bruker Nano Surfaces Division Santa Barbara, CA • USA +1.805.967.1400/800.873.9750 productinfo@bruker-nano.com
www.bruker.com
6. Busbee B.D., Obare S.O, Murphy C.J. (2003). **An Improved Synthesis of High-Aspect-Ratio Gold Nanorods.** Adv. Mater., 15: 414–416. doi: 10.1002/adma.200390095
7. Caswell K.K, Bender C.M, and Murphy C.J; (2003) **Seedless and Surfactantless Wet Chemical Synthesis of Silver Nanowires.** American Chemical Society
Published on Web 04/22/2003
8. C Xue, G S. Metraux, J E. Millstone, and C A. Mirkin; (2008) **Mechanistic Study of Photomediated Triangular Silver Nanoprism Growth.** J. AM. CHEM. SOC, 130, 8337–8344

9. Deivaraj T.C, Lala N.L, Lee J.Y; (2005) **Solvent-induced shape evolution of PVP protected spherical silver nanoparticles into triangular nanoplates and nanorods.** Journal of Colloid and Interface Science 289 402–409
10. **Formulation for Dulbecco's Modified Eagle's Medium (DMEM)** ATCC® 30-2002; P.O. Box 1549 Manassas, VA 20108 USA www.atcc.org
11. Ghosh S K and Pal T; (2007) **Interparticle Coupling Effect on the Surface Plasmon Resonance of Gold Nanoparticles: From Theory to Applications.** Chem. Rev. 107, 4797-4862
12. Gupta K.A, Gupta M; (2005), **synthesis and surface engineering of iron oxide nanoparticles for biomedical applications.** Volume 26, Issue 18, Pages 3995–4021
13. Goebel J., Zhang Q., He L. and Yin Y. (2012), **Monitoring the Shape Evolution of Silver Nanoplates: A Marker Study.** Angew. Chem. Int. Ed., 51: 552–555. doi: 10.1002/anie.201107240
14. Heckmann L H and Connon R; (2007) **Culturing of Daphnia magna - Standard Operating Procedure.** Daphnia Research group (University of Reading) Last updated <http://www.biosci.rdg.ac.uk/Research/eb/daphnia.html>
- Jin R; (2001) **Photoinduced Conversion of Silver Nanospheres to Nanoprisms** DOI: 10.1126/science.1066541 Science 294, 1901.
15. Jana N.R, Gearheart .L and Murphy C.J. (2001) **Wet chemical synthesis of silver nanorods and nanowires of controllable aspect ratio.** Chem Commun., 617–618
16. Jin R, Qian. H, Wu .Z, Zhu Y, Zhu M, Mohanty A, Garg N; (2010). **Size focusing: A methodology for synthesizing atomically precise gold nanoclusters.** Journal of Physical Chemistry Letters, Issue 1, 2903-2910.
17. Jin, R., Cao, Y., Mirkin, C. A., Kelly, K. L., Schatz, G. C., & Zheng, J. G. (2001). **Photoinduced conversion of silver nanospheres to nanoprisms.** Science, 294(5548), 1901-1903

18. Junior A.M, Oliveira H.P and Gehlen M.H; (2003) **Preparation of silver nanoprisms using poly(N-vinyl-2-pyrrolidone) as a colloid-stabilizing agent and the effect of silver nanoparticles on the photophysical properties of cationic dyes.** Photochem. Photobiol. Sci., 2, 921–925
19. Li H. W, Yang C. C, Tsao C. F, Lee C. K; (2003), **Quantum size effects on the superconducting parameters of zero-dimensional Pb nanoparticles.** Phys. Rev. B 68, 184507, Issue 18
20. Lok N.C, Ho M.C, Chen R, He Y.Q, Yu Y.W, Sun H, Tam H.K.P, Chiu F.J, Che M.C; (2007). **Silver nanoparticles: partial oxidation and antibacterial activities.** JBIC Journal of Biological Inorganic Chemistry, May 2007, Volume 12, Issue 4, pp 527-534
21. Maretti L, Billone S.P, Liu Y, Scaiano C.J; (2009). **Facile photochemical synthesis and characterization of highly fluorescent silver nanoparticles.** Journal of American Chemical Society, 131, 13972-13980
22. Morones Lovern S B, Owen H.A, and Klaper R; (2008) **Electron microscopy of gold nanoparticle intake in the gut of Daphnia magna.** Nanotoxicology 2:1, 43-48
23. Morita S, Wiesendanger R, Meyer E; (1995), **Noncontact Atomic Force Microscopy, Volume 1.** Nanoscience and Technology, Springer
24. Malynych S and Chumanov G; (2003) **Light-Induced Coherent Interactions between Silver Nanoparticles in Two-Dimensional Arrays.** J. AM. CHEM. SOC. 125, 2896-2898
25. Métraux G. S, Mirkin, C. A. (2005). **Rapid Thermal Synthesis of Silver Nanoprisms with Chemically Tailorable Thickness.** Adv. Mater., 17: 412–415. doi: 10.1002/adma.200401086

26. Metraux G.S, Cao Y C, Jin R, and Mirkin C.A; (2003) **Triangular Nanoframes Made of Gold and Silver**. Nano Letters, Vol. 3, No. 4 519-522.
27. Millstone J.E, Hurst J.S, Me´traux S.G, Cutler I J, and Mirkin C A; (2009), **Colloidal Gold and Silver Triangular Nanoprisms**. Inter science Wiley journal small, 5, No. 6, 646–664
28. Murphy C.J, Gole M.A, Hunyadi E.S, Stone W.J, Sisco N.P , Alkilany A , Kinard E.B and Hankins P; (2007). **Chemical sensing and imaging with metallic nanorods**. Chem. Commun., 2008, 544-557 DOI: 10.1039/B711069C
29. R.J, Elechiguerra L.J, Camacho A, Holt K, Kouri B.J, Jose Ram´ırez T, Yacaman J.M; (2005). **The bactericidal effect of silver nanoparticles**. Nanotechnology 16 2346 doi:10.1088/0957-4484/16/10/059
30. Petersen E J, Akkanen J, Kukkonen J V. K, and Weber W J Jr, (2009) **Biological Uptake and Depuration of Carbon Nanotubes by Daphnia magna**. Environmental Science & Technology 43 (8), 2969-2975
31. Rosenkranz, P., Chaudhry, Q., Stone, V. and Fernandes, T. F. (2009), **A comparison of nanoparticle and fine particle uptake by Daphnia magna**. Environmental Toxicology and Chemistry, 28: 2142–2149. doi: 10.1897/08-559.1
32. Sherry J.L, Jin. R, Mirkin C.A, Schatz G.C, Duyne V.P.R **Localized Surface Plasmon Resonance Spectroscopy of Single Silver Triangular Nanoprisms** Nano Letters 2006 6 (9), 2060-2065
33. Sun.Y, Xia.Y, (2002). **Shape-controlled synthesis of gold and silver Nanoparticles**. Science 13 December, Vol. 298 no. 5601 pp. 2176-2179 DOI: 10.1126/science.1077229
34. Sun .Y; (2002) **Shape-Controlled Synthesis of Gold and Silver Nanoparticles**. DOI: 10.1126/science.1077229 Science 298, 2176

35. Volokitin Y, Sinzig J, Jongh de J L, Schmid G, Vargaftik M K, Moiseevi I I; (1996), **Quantum-size effects in the thermodynamic properties of metallic nanoparticles.** Nature 384, 621-623
36. Sun, Y., Mayers, B., Herricks, T., & Xia, Y. (2003). **Polyol synthesis of uniform silver nanowires: a plausible growth mechanism and the supporting evidence.** Nano Letters, 3(7), 955-960
37. Wei Q, Yu L, Mather R R, Wang X; (2007), **preparation and characterization of titanium dioxide nanocomposite fibers.** Journal of Materials Science, Volume 42, Issue 19, pp 8001-8005
38. Wulff G, Kristallogr Z; (1901) **on the question of the speed of growth and resolution of the crystal faces,** 34, 449
39. Wiley J.B, Sun Y, Xia Y; (2005) **Polyol synthesis of silver nanostructures: control of product morphology with Fe (II) or Fe (III) species.** Langmuir, 21, 8077.
40. Wiley J.B, Herricks T, Sun Y, Xia Y; (2004) **Polyol Synthesis of Silver Nanoparticles: Use of Chloride and Oxygen to Promote the Formation of Single-Crystal, Truncated Cubes and Tetrahedrons.** Nano Lett., 4, 1733.
41. Wiley J.B, Sun Y, Mayers B, and Xia Y; **Shape-Controlled Synthesis of Metal Nanostructures: The Case of Silver;** Chem. Eur. J. 2005, 11, 454 – 463
42. Wiley J.B, Wang Z, Wei.J, Yin.Y, Cobden D.H, and Xia .Y; (2006) **Right Bipyramids of Silver: A New Shape Derived from Single Twinned Seeds.** Nano Lett., 6, 2273
43. Xie J, Lee J Y, Daniel I and Ting Y P; (2007) **Silver Nanoplates: From Biological to Biomimetic Synthesis.** VOL. 1 ▪ NO. 5 ▪ 429–439
44. Xiong, Y., Wiley J.B, Chen, J., Li, Z.-Y., Yin, Y. and Xia, Y. (2005), **Corrosion-Based Synthesis of Single-Crystal Pd Nanoboxes and Nanocages and Their**

- Surface Plasmon Properties.** Angew. Chem., 117: 8127–8131. doi: 10.1002/ange.200502722
45. Xue C and Mirkin C.A; (2007) **pH-Switchable Silver Nanoprism Growth Pathways** Angew. Chem. 119, 2082 –2084
46. Xia, Y., Yang, P., Sun, Y., Wu, Y., Mayers, B., Gates, B., Yin, Y., Kim, F. and Yan, H. (2003), **One-Dimensional Nanostructures: Synthesis, Characterization, and Applications.** Adv. Mater., 15: 353–389. doi: 10.1002/adma.200390087
47. Xue C, Mirkin C A. (2007). **pH-Switchable Silver Nanoprism Growth Pathways.** Angew. Chem., 119: 2082–2084. doi: 10.1002/ange.200604637
48. Yang, H., Zhu, S. and Pan, N. (2004), **Studying the mechanisms of titanium dioxide as ultraviolet-blocking additive for films and fabrics by an improved scheme.** J. Appl. Polym. Sci., 92: 3201–3210. doi: 10.1002/app.20327
49. Yujie. X; Jingyi .C; Wiley J.B; Xia. Y; Shaul .A; Y. Yadong .Y. (2005) **Understanding the role of oxidative etching in the polyol synthesis of Pd nanoparticles with uniform shape and size.** Journal of the American Chemical Society, 127(20), 7332-7333 CODEN: JACSAT; ISSN: 0002-7863.
50. Zhang Q, Li N, Goebel J, Lu Z and Yin. Y; (2011) **Systematic Study of the Synthesis of Silver Nanoplates: Is Citrate a “Magic” Reagent.** Am. Chem. Soc. 133, 18931–18939
51. **Zetasizer Nano Series User Manual.** MAN 0317 Issue 1, 1 Feb. 2004 Malvern Instruments Ltd. 2003, 2004
52. Zhao M. C and Wan X. W; (2010) **Size-Dependent Uptake of Silver Nanoparticles in Daphnia magna.** Environmental Science & Technology 46 (20), 11345-11351
53. Zhao M.C, Wang X. W; (2010), **Biokinetic Uptake and Efflux of Silver Nanoparticles in Daphnia magna.** Environmental Science & Technology 44 (19), 7699-7704

54. Zhang Q, Li N, Goebel J, Lu Z, Yin Y. (2011) **a Systematic Study of the Synthesis of Silver Nanoplates: Is Citrate a “Magic” Reagent?** J. Am. Chem. Soc. 133, 18931–18939
55. Zhang, Q., Hu, Y., Guo, S., Goebel, J., & Yin, Y. (2010). **Seeded growth of uniform Ag nanoplates with high aspect ratio and widely tunable surface plasmon bands.** Nano letters, 10(12), 5037-5042.